ELSEVIER

Contents lists available at ScienceDirect

Chemical Geology

journal homepage: www.elsevier.com/locate/chemgeo





U-Pb and Lu-Hf isotopic evolution of \sim 3.6 Ga remnants in NE Brazil – Implications on Eo-Paleoarchean global crustal evolution

Manuela Botero ^{a,*}, Jeffrey D. Vervoort ^a, Vinicius T. Meira ^b, Daniel F. Martins de Sousa ^b, Ticiano J.S. Santos ^b

ARTICLE INFO

Keywords:
Paleoarchean
U-Pb geochronology
Hf isotopes
São Francisco Craton
Borborema Province
Global Hf isotope record.

ABSTRACT

Precambrian terrains preserving rocks older than 3.5 Ga contain an essential record of the crustal evolution of the primitive Earth. In this study, we investigated Eo-Paleoarchean rocks from the northern São Francisco Craton (NSFC) and the Borborema Province in northeastern Brazil to contribute to a more complete global isotopic record of this pivotal time in Earth's history. Zircon U-Pb ages along with zircon Hf isotope compositions were obtained for migmatitic gneiss complexes in both terrains. Zircon U-Pb data from the NSFC yield well-defined populations with $^{207}\text{Pb}/^{206}\text{Pb}$ ages from 3.61 to 3.59 Ga and younger components at $\sim\!3.5$ and $\sim\!3.4$ Ga. Similarly, the Borborema Province gneiss yields a main zircon age population of 3.58 Ga and a younger $\sim\!3.5$ Ga age component. The $\sim\!3.6$ Ga zircon components yield consistently sub-chondritic Hf isotopic compositions with initial $\epsilon_{\rm Hf}$ between -1.9 and -3.1 for the NSFC and of $\epsilon_{\rm Hf}$ -0.5 for the Borborema Province. Gneisses from northeastern Brazil record a main crust forming period at 3.65–3.60 Ga with sub-chondritic Hf isotope compositions that indicate derivation from melting of a $\sim\!3.8$ Ga source of broadly chondritic isotope composition, similar to that of many Eo-Paleoarchean gneisses worldwide. This Hf isotope record supports the existence of broadly chondritic mantle reservoir in the Eoarchean with development of depleted mantle and the appearance of evolved crust later in the Paleoarchean.

1. Introduction

The nature, extent, and mechanisms driving the growth of the continental crust in the early history of the Earth remain highly debated. Models for crustal growth in Earth's early history fall into two endmember scenarios: The first proposes that continental crust formed early in the Hadean (often called the no-growth model), with volumes similar to those of the present-day (e.g., Armstrong, 1991; Bowring and Housh, 1995; Harrison et al., 2005; The second suggests progressive crustal production over time, with significant volumes only forming since the Eoarchean (e.g., McLennan and Taylor, 1982; Patchett and Arndt, 1986). Archean cratons worldwide, which comprise about 7 % of the present-day crustal volume (e.g., Bleeker, 2003), preserve the rock record of Earth's early history. This record shows a nearly total absence of Hadean crust with increasing abundance from the Eoarchean to the Paleoarchean. This sparse ancient rock record supports the progressive crustal growth model. Proponents of the no-growth model, however,

argue that the lack of rock record from the first ~500 million years of Earth's history, can be attributed to the effective destruction and recycling of continental crust into the mantle during this time (e.g., Armstrong, 1991; Bowring and Housh, 1995; Harrison et al., 2005). Whether the Eo-Paleoarchean crust represents increased crustal production (Condie, 2000; Condie and Aster, 2010; Patchett and Arndt, 1986) or enhanced crustal preservation (Cawood et al., 2013; Hawkesworth et al., 2013; Hawkesworth et al., 2009; Hawkesworth et al., 2017) remains a matter of considerable debate. The long-lived Lu-Hf and Sm-Nd isotope systems have long been employed to unravel the complex geological record of Eo-Paleoarchean remnants, with particular focus on Precambrian terrains such as the Kaapvaal and Pilbara cratons, the Acasta gneiss complex, and west Greenland gneisses. The rock record of relatively understudied Precambrian terrains is crucial to this discussion. Incorporating data from these terrains will help build a more complete global isotope record which, in turn, will improve our understanding of mantle differentiation and crustal evolution in Earth's early history.

E-mail address: manuela.botero@wsu.edu (M. Botero).

^a School of the Environment, Washington State University, Pullman, WA 99164, USA

^b Institute of Geosciences, University of Campinas, Campinas, São Paulo, Brazil

^{*} Corresponding author.

The Paleoarchean is a pivotal period in Earth's evolution relevant to the question of crustal growth as it is marked by the emergence of significant volumes of continental crust in the geological record. In this way, it provides crucial information to understand the formation of stable continental crust, mantle differentiation, and transitions in geodynamic modes (e.g., Cawood et al., 2022). Rocks older than 3.5 Ga are preserved either as first additions of juvenile material or as reworked crust in scattered locations on Earth (Fig. 1). Juvenile additions are exposed in many locations including west Greenland (e.g., Fisher and Vervoort, 2018; Kemp et al., 2019), the Pilbara (e.g., Kemp et al., 2023; Petersson et al., 2020; Salerno et al., 2021), and Kaapvaal (e.g., Amelin et al., 2000; Hoffmann et al., 2016; Laurent and Zeh, 2015; Moyen et al., 2021; Zeh et al., 2009) cratons. Hadean detrital zircon from the Jack Hills locality and Eoarchean zircon from the Acasta Gneiss complex, on the other hand, record reworking of pre-existing crust (e.g., Bauer et al., 2017; Iizuka et al., 2009; Kemp et al., 2010). The Hf isotope record of juvenile additions are mostly chondritic in composition (e.g., Fisher and Vervoort, 2018; Kemp et al., 2023; Kemp et al., 2010; Vervoort and Kemp, 2025) while zircon indicating crustal reworking are characterized by sub-chondritic Hf isotopes with progressively more negative isotope compositions over time (e.g., Bauer et al., 2017; Kemp et al., 2010; Mulder et al., 2021). Lack of super-chondritic Hf isotope compositions of Hadean-Eoarchean remnants has been used to argue against the existence of extensive depleted mantle sources and Hadean evolved crust (e.g., Fisher and Vervoort, 2018; Kemp et al., 2023, Kemp et al., 2010; Vervoort and Kemp, 2025). Precambrian terranes such as the Slave, Wyoming, and Yilgarn cratons exhibit shifts in the Hf isotope record from dominantly crustal reworking signatures to the appearance of juvenile additions that have been linked to changes in geodynamic regimes (e.g., Mulder et al., 2021). Such isotopic shifts, however, are not observed in all Precambrian terrains, and where they do occur, their timing varies between cratons, suggesting localized geodynamic changes rather than a global tectonic transition (e.g., Kemp et al., 2023; Laurent et al., 2024).

In this study, we integrate zircon U-Pb and Hf isotope data with bulk-rock geochemistry to study Eo-Paleoarchean remnants from the northern São Francisco Craton and Borborema Province in northeastern Brazil. The U-Pb and Hf isotope data obtained in this study allow us to place Paleoarchean crustal evolution of northeastern Brazil and contribute to a more representative record of Paleoarchean magmatic

events by filling gaps in the global isotope record.

2. Geological overview

The northern São Francisco Craton (NSFC) in northeastern Brazil, exposes several Archean to Paleoproterozoic units that were assembled during the Neoarchean and mid-Paleoproterozoic (e.g., Barbosa and Barbosa, 2017; Barbosa and Sabaté, 2004; Martins de Sousa et al., 2020; Oliveira et al., 2020; Teixeira et al., 2017). Archean blocks within the NSFC, including the Gavião, Jequié, and Serrinha blocks (Fig. 2), are primary composed of closely related tonalite-trondhjemite-granodiorite (TTG) rocks and granite-greenstone associations (e.g., Teixeira et al., 2017). The 3.64-3.60 Ga low to medium pressure TTG gneisses of the Mairi Complex within the Gavião Block are the oldest rocks that have been dated in the South America continent (Moreira et al., 2022; Oliveira et al., 2020). Magmatic events late in the Paleoarchean (3.4–3.2 Ga) and in the Neoarchean (2.80-2.56 Ga) are also recorded within the Gavião Block (e.g., Barbosa et al., 2013; dos Santos et al., 2022; Medeiros et al., 2017; Teixeira et al., 2017; Zincone et al., 2016). Archean crust in the NSFC experienced high-grade metamorphism and crustal reworking during the Paleoproterozoic in what has been called the Itabuna-Salvador-Curacá orogeny (ISCO, Fig. 2) (e.g., Martins de Sousa et al., 2020; Teixeira et al., 2017). This Paleoproterozoic orogenic event is thought to have been the main driver of the amalgamation of the Archean blocks in the NSFC (e.g., Teixeira et al., 2017; Barbosa and Barbosa, 2017).

The Borborema Province is a late Neoproterozoic orogenic system associated with the assembly of Gondwana (e.g., de Almeida et al., 2011; Ganade de Araujo et al., 2014). This orogenic system surrounds the São Francisco Craton to the northeast and includes Archean inliers in its basement (Fig. 2), such as dismembered greenstones and ancient TTG rocks, possibly representing crustal reworking of the craton (e.g., Ganade et al., 2021; Neves, 2003). Paleoproterozoic (2.5–2.0 Ga) migmatitic gneisses dominate the basement exposures throughout the province (e.g., Neves, 2015; Fig. 2). Enclaves of Archean (~3.5 and ~3.2 Ga) tonalitic to monzogranitic gneisses are surrounded by Paleoproterozoic orthogneisses and Meso- to Neoproterozoic supracrustal sequences (e.g., Dantas et al., 2004, 2013; Fachetti et al., 2024; Ferreira et al., 2020; Pitarello et al., 2019). Pervasive magmatism and shearing associated with the development of a continental-scale strike-slip shear

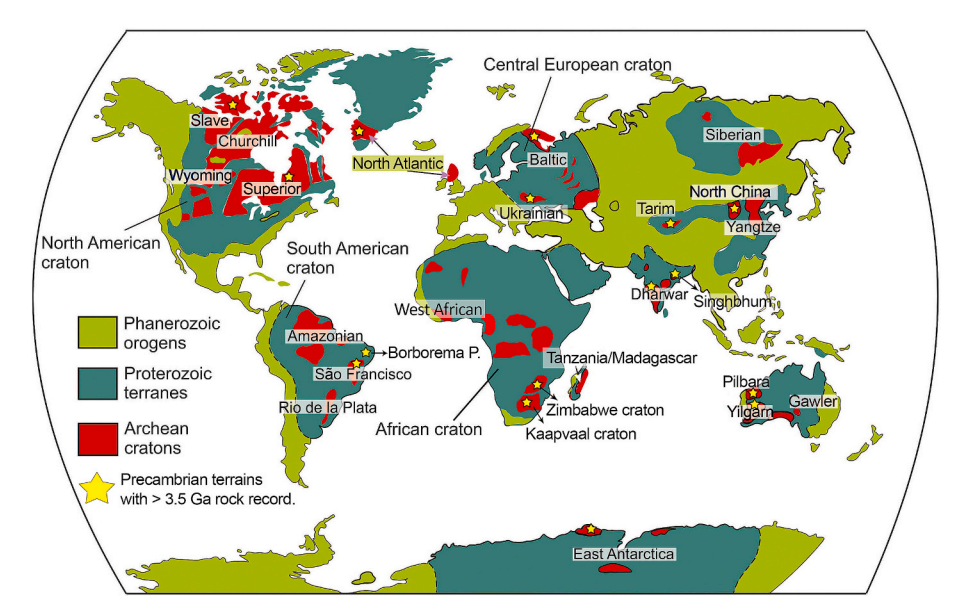


Fig. 1. World map showing distribution of major Precambrian terranes and Phanerozoic orogens after Groves and Santosh (2021). Precambrian terranes with preserved rocks >3.5 Ga are shown with a yellow star. (For interpretation of the references to color in this figure legend, the reader is referred to the web version of this article.)

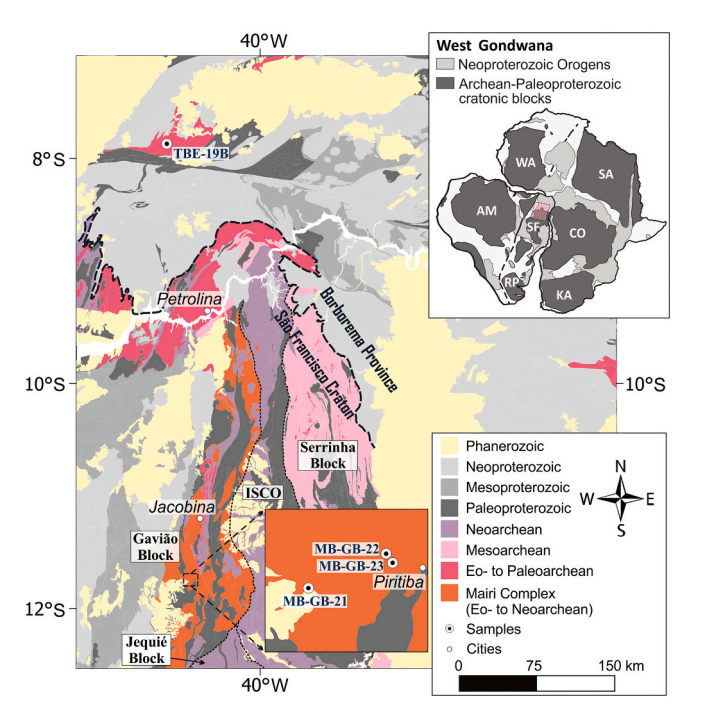


Fig. 2. Simplified sketch of West Gondwana (adapted after Schmitt et al., 2018) and geological map of the northern São Francisco craton and Borborema Province (modified from Delgado et al., 2021) showing the locations of samples analyzed in this study. ISCO: Itabuna Salvador Curaçá Orogen. The tectonic boundary between the São Francisco craton and Borborema Province is shown with a thick dashed black line. AM: Amazonian Craton; SF: São Francisco Craton; RP: Rio de la Plata Craton; WA: West African Craton; CO: Congo Craton; KA: Kalahari Craton; SA: Sahara Craton.

zone system affected the province during the 0.60–0.56 Ga time interval (e.g., Neves, 2021).

3. Samples and Analytical techniques

3.1. Samples

A total of 10 samples from migmatitic gneiss complexes within the Gavião Block in the northeastern part of the São Francisco Craton as well as one banded gray gneiss from the western part of Borborema Province (Fig. 2), were analyzed in this study. A detailed description of individual samples is given in the Supplementary materials. Samples from the northern São Francisco Craton were collected from three outcrops (MB-GB-21, MB-GB-22, and MB-GB-23) within the Mairi Complex, located in the northern part of the Gavião Block near the city of Piritiba (inset in the Fig. 2). We used a cordless cut-off saw in the field to obtain fresh, single-phase rock specimens from migmatitic complexes. The MB-GB-21 group of samples are different phases of a migmatitic-gneiss complex from a single outcrop (Fig. 3a-e). This large and continuous outcrop exposes tightly folded banded gray gneisses with evidence of partial melting (metatexites; Figs. 3a-e) and local exposures of transitional metatexite-diatexite rocks (Fig. 3b,d), as well as intrusive leucosomes (Fig. 3d). The analyzed samples include a massive medium-grained granitoid (MB-GB-21A, Fig. 3b) with pervasive K-feldspar veining from a felsic band in the banded gneiss, a pyroxene-rich mafic band of dioritic composition (MB-GB-21B; Fig. 3c), three fine-banded gray gneisses (MB-GB-21C, MB-GB-21D, and MB-GB-21F; Fig. 3a,d,e), and a biotite granitoid from a leucosome phase (MB-GB-21E; Fig. 3d). The dominant phase of the outcrop, the gray banded gneiss, shows variations in grain size from medium- to coarse-grained with millimeter to centimeter thick felsic and mafic bands (Fig. 3a-e). Two samples collected from the MB-GB-22 outcrop are a residue rich phase of dioritic



Fig. 3. Representative images from outcrops where samples were collected for this study.

composition (MB-GB-22A; Fig. 3g) and a gray gneiss (MB-GB-22B; Fig. 3f). A massive tonalite (MB-GB-23A; Fig. 3i), and a gray gneiss (MB-GB-23C; Fig. 3h) from a third location were also collected and analyzed. The sample from the Borborema Province is a banded gneiss (TEB-19b) of trondhjemitic composition with evidence of shear deformation (Fig. 3j) collected in the western part of the province (Fig. 2).

3.2. Analytical techniques

In this study we combine zircon U-Pb dating with Lu-Hf isotopes from zircon along with bulk-rock chemistry. Methods used in this study are described in detail in the supplementary materials. Mineral separation and rock powdering of samples from the northern São Francisco Craton were performed at Zirchron LLC, Tucson, AZ using an Electro Pulse Disaggregator (EPD, Marx generator) and Spex mill with silica grinding balls, respectively. Zircon separates from the Borborema Province gneiss were obtained in Brazil at the University of Campinas. Mineral mounts and isotopic analyses were performed in-house at the Radiogenic Isotope and Geochronology Laboratory (RIGL) at Washington State University.

Uranium-Pb and Hf in-situ measurements were obtained from zircon grains through laser ablation-inductively coupled plasma mass spectrometry (LA-ICPMS) and by the laser ablation split stream (LASS) method. With LASS, two individual mass spectrometers, the Element2 HR-MS-ICPMS and Neptune Plus MC-ICPMS, are connected to simultaneously determine the U-Pb dates and Hf isotopic composition from the same volume (e.g., Fisher et al., 2014). The U-Pb and Hf isotopes data were reduced using the "U-Pb Geochronology" and "Hf Isotopes" data

reduction schemes, respectively, within Iolite v4 (Paton et al., 2011; Paton et al., 2010).

Reference materials were analyzed along with unknowns—typically a set of standards for every 10 unknowns. For zircon U-Pb, the FC1 (1099 Ma; Paces and Miller, 1993) and Plešovice (337.1 Ma; Sláma et al., 2008) standards were used as principal reference materials to correct for $^{207} {\rm Pb}/^{206} {\rm Pb}$ and $^{206} {\rm Pb}/^{238} {\rm U}$, respectively. Secondary zircon reference materials including the 91500 (1065 Ma; Wiedenbeck et al., 1995), OGC-1 (3465.4 Ma; Stern et al., 2009), and GJ-1 (609 Ma; Jackson et al., 2004) were used to evaluate the accuracy of the analyses during each analytical session. The U-Pb data from reference materials are reported in Table S4. The U-Pb ages obtained for each zircon standard in different analytical sessions are within $\sim \! \! 1$ % of their reported "true" age and are shown in Figs. S1-S3 of supplementary materials

For the Lu-Hf isotope analytical sessions we analyzed natural zircon standards and synthetic zircons MUNZirc along with unknowns in a similar way as described above for U-Pb analytical sessions. The calibrated synthetic zircons with a large range of REE/Hf (MUNZirc; Fisher et al., 2011) were analyzed to monitor the correction for isobaric interferences of ¹⁷⁶Yb and ¹⁷⁶Lu on ¹⁷⁶Hf. The MUNZirc 142 and 144 standards as well as natural zircon and unknowns vielded homogeneous ¹⁷⁶Hf/¹⁷⁷Hf isotope ratios through the ¹⁷⁶Yb/¹⁷⁷Hf range (Tables S2 and S5, Figs. S4 and S5) validating the interference correction. Following mass-bias and interference corrections, the ¹⁷⁶Hf/¹⁷⁷Hf isotope ratios of unknowns were normalized to the Plešovice zircon standard ($^{176} {\rm Hf}/^{177} {\rm Hf} = 0.282482 \pm 13;$ Sláma et al., 2008). A mean $^{176} {\rm Hf}/^{177} {\rm Hf}$ of 0.282482 \pm 22 was obtained for the Plešovice standard during both single stream (LA-ICPMS) and split stream (LASS) analytical sessions (Table S5). Secondary reference materials including OGC-1 (Kemp et al., 2017), FC1 (Fisher et al., 2014), and 91500 (Blichert-Toft, 2008) yielded Hf isotope compositions within 1 epsilon unit of the reported values (Table S5 and Fig. S6).

Bulk-rock geochemistry was performed at the Peter Hooper Geo-Analytical Lab using X-Ray fluorescence (XRF) and ICP-MS. The long-term precision for the geochemistry data is $\sim\!1$ % for La, Ce, Pr, Nd, Gd, Tb, Dy, Ho, Y, Hf, Sc, and Zr; $\sim\!2$ % for Sm, Eu, Er, Tm, Yb, Ba, Th, Nb, Ta, Cs, and Sr; $\sim\!3$ % for Lu; and $\sim\!4\!-\!6$ % for U, Pb, Rb (Steenberg et al., 2017). Major and trace element data from bulk-rock samples are reported in Table S3 and Figs. S7-S9.

4. Results

The U-Pb and Hf isotope results from this study are summarized in Table 1 and presented in Figs. 4 to 7. Detailed results are reported in supplementary Tables S1 and S5. Results are briefly described in the following section, only highlighting special cases. For more detailed descriptions of the results the reader is referred to the supplementary materials.

4.1. Bulk-rock major and trace element chemistry

Bulk-rock compositions in this study span a wide range of silica content from 51 to 73 % with the lowest SiO₂ percentages determined for residue rich phases MB-GB-21B and MB-GB-22A (Table S3). Most samples have low K_2O (0.8–1.7 %) and high Na_2O (4.8 to 7.5 %) with K_2O/Na_2O < 0.5 (Table S3). The residue rich MB-GB-22A has a lower Na_2O content of 2.6 % with K_2O/Na_2O of 0.15 (Table S3). Gray gneisses MB-GB-21C and MB-GB-21F and residue rich phases MB-GB-21B and MB-GB-22A have high concentrations of ferromagnesian oxides (FeO + MgO + MnO + TiO₂ > 5 %) and CaO (CaO between 5 and 9 %) relative to the other samples with ferromagnesian oxides <5 % and CaO content <4 % (Table S3). Low Ce/Sr ratios (0.5–0.1), Th below 15 ppm, and variable Y (55–2 ppm) are commonly observed in bulk rocks in this study (Table S3). Additionally, most samples have light-REE (LREE) enrichment relative to heavy-REE (HREE) with La/Yb generally >10 and absent or minor negative Eu anomalies (Eu/Eu* between 0.7 and 1.0) in

Table 1
Summary of the zircon U-Pb and Lu-Hf isotope results reported in this study.

Sample	Latitude	Longitude	Age \pm 2 SE (Ma)	$\epsilon_{Hf(i)}$	$\pm \; 2\; SD$
MB-GB-21 A: Massive granitoid					
	-11.751878	-40.642128	3590 ± 6	-1.9	± 1.6
			3517 ± 11	+0.2	± 1.4
MB-GB-21B: Residue rich dioritic phase					
	-11.751878	-40.642128	3598 ± 5	-2.4	$\pm~1.7$
MB-GB-21C: Gray gneiss					
	-11.751878	-40.642128	3593 ± 7	-3.1	$\pm~1.7$
MB-GB-21D: Gray gneiss					
	-11.751878	-40.642128	3593 ± 5	-2.4	$\pm~1.8$
MB-GB-21E: Leucosome					
	-11.751878	-40.642128	3593 ± 7	-2.5	± 1.6
			3482 ± 8	-3.2	$\pm~1.5$
MB-GB-21F: Gray gneiss					
	-11.751878	-40.642128	3612 ± 7	-2.9	± 1.0
MB-GB-22B: Gray gneiss					
	-11.735144	-40.587633	3413 ± 6	-2.9	± 1.9
			3602 ± 15	-2.6	$\pm~0.8$
MB-GB-23 A: Massive tonalite					
	-11.735878	-40.585936	3515 ± 20	+0.7	$\pm~1.9$
			3698 ± 25	-0.5	$\pm~0.8$
MB-GB-23C: Gray gneiss					
	-11.735878	-40.585936	3592 ± 9	-2.4	$\pm~2.0$
TBE-19b: Gray gneiss					
	-7.859776	-40.828594	3577 ± 11	-0.5	± 1.5
			3487 ± 14	_	_

Initial Hf isotope compositions are calculated at the zircon U-Pb age and are reported as $\epsilon_{\rm Hf(i).}$

Initial compositions were calculated using the Lu decay constant of Scherer et al. (2001) and Söderlund et al. (2004) (λ^{176} Lu = 1.867 × 10⁻¹¹ y⁻¹).

The Lu-Hf isotope compositions of CHUR of Bouvier et al. (2008) were used to obtain epsilon values.

chondrite normalized REE plots (Fig. S7). Two samples, MB-GB-21A and MB-GB-21E, exhibit REE patterns that differ from the general trend of most samples. The massive granitoid MB-GB-21A shows a more fractionated REE pattern and lower total REE in comparison to the rest of the samples as well as strong positive Eu anomaly (Fig. S7). The leucosome (MB-GB-21E) exhibits the least fractionated REE pattern (La/Yb = 0.8) with slight depletion in both LREE and HREE and weak negative Eu anomaly (Fig. S7).

4.2. Zircon U-Pb geochronology

Zircon separates were obtained from all samples in this study except for the residue rich phase MB-GB-22A (Tables 1 and S1). In-situ zircon U-Pb dates from NSFC samples can be placed in two groups. The first group with zircon U-Pb dates ranging from 3.61 Ga to 3.59 Ga (Fig. 4), and the second group with zircon U-Pb dates that range from 3.52 Ga to 3.41 Ga (Fig. 5). Within the first group, concordant to slightly reverse discordant analyses define main zircon ~3.6 Ga populations in 5 samples (Fig. 4). The dioritic band (MB-GB-21B), gray gneiss (MB-GB-21D), and granitoid (MB-GB-21A) yielded Concordia ages of 3598 \pm 5 Ma (n = 6, MSWD = 1.2; Fig. 4a), 3593 ± 5 Ma (n = 7, MSWD = 1.0; Fig. 4B), and 3590 \pm 6 Ma ($\it n=5$, MSWD = 1.4; Fig. 4c), respectively. Weighted mean $^{207}\text{Pb}/^{206}\text{Pb}$ ages (WMA) of 3593 \pm 7 Ma (n=10, MSWD =1.0) and 3612 ± 7 Ma (n = 10, MSWD = 1.3) were calculated from concordant to slightly reverse discordant analyses for gray gneisses MB-GB-21F (Fig. 4d) and MB-GB-21C (Fig. 4e), respectively. The main \sim 3.6 Ga population in the gray gneiss MB-GB-23C is defined by variably concordant and discordant analyses plotting along a Discordia line with an upper intercept at 3592 \pm 9 Ma (n=15, MSWD =1.3; Fig. 4f). The leucosome MB-GB-21E yields concordant and discordant analyses that define a \sim 3.6 Ga component with an upper intercept age of 3593 \pm 7 Ma for this sample (n = 12, MSWD = 1.6; Fig. 5a).

Within the second group, the leucosome MB-GB-21E yields variably concordant to discordant analyses defining a linear regression with

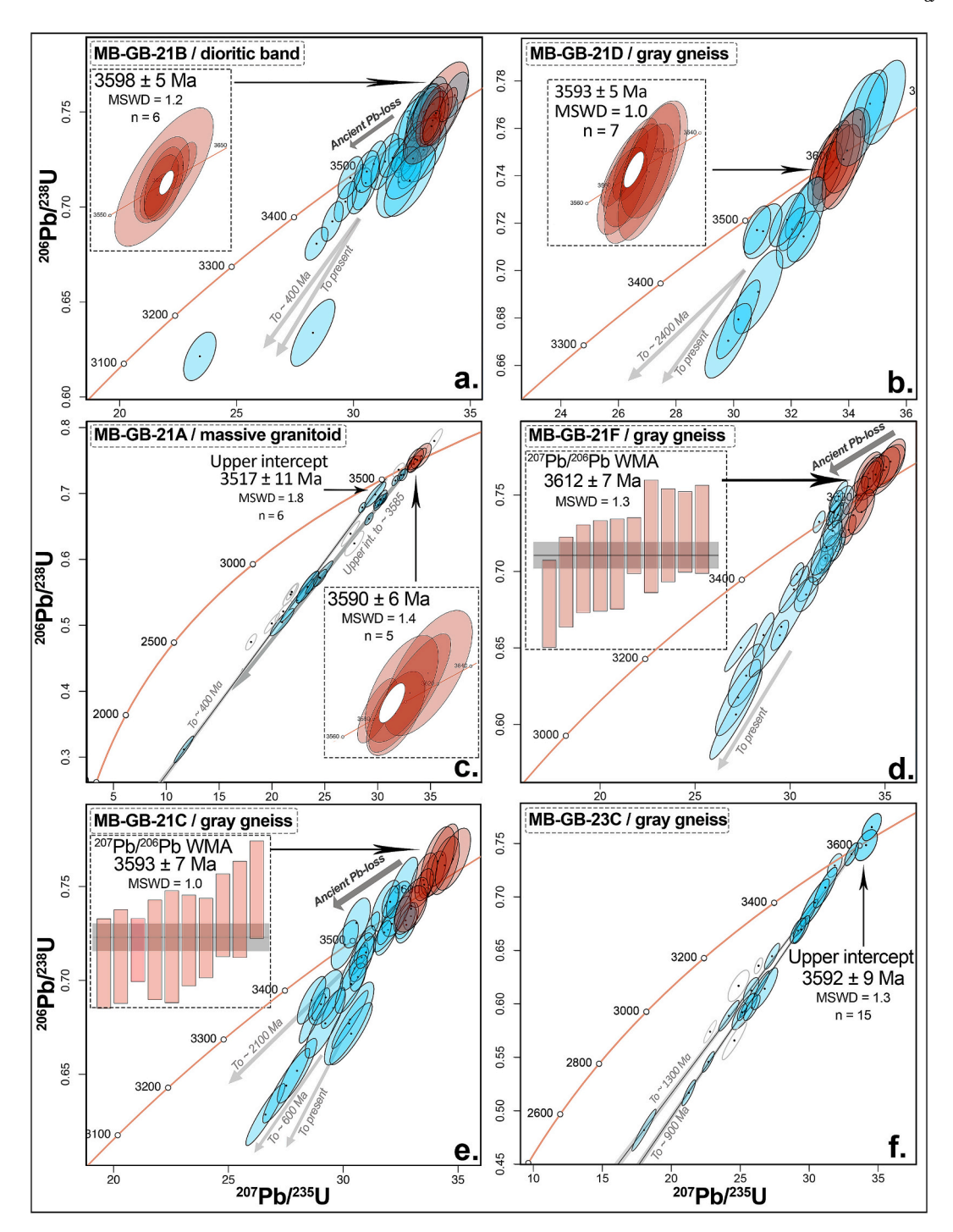


Fig. 4. Zircon U-Pb data from samples of the NSFC with main zircon age populations of ~3.6 Ga. (a) MB-GB-21B, (b) MB-GB21D, (c) MB-GB-21A, (d) MB-GB-21F, (e) MB-GB-21C, and (f) MB-GB-23C.

upper intercept at 3482 \pm 8 Ma (n=13, MSWD =1.4; Fig. 5a). The tonalite MB-GB-23A yields only discordant analyses that define a linear regression with an upper intercept of 3515 ± 20 Ma (n=11, MSWD =1.7; Fig. 5b). Concordant analyses of the gray gneiss MB-GB-22B define a Concordia age of 3413 ± 6 Ma (n=8, MSWD =1.1; Fig. 5c). The massive tonalite, MB-GB-21A, with a main zircon population of ~ 3.6 Ga, yields an upper intercept age of 3517 ± 11 Ma (n=6, MSWD =1.8; Fig. 4c) defined by variably discordant analyses. Inheritance occurs in two samples in this study (MB-GB-22B and MB-GB-23A). Three concordant to slightly discordant analyses define a 207 Pb/ 206 Pb WMA of 3602 ± 15 Ma in sample MB-GB-22B (n=3, MSWD =2.2; Fig. 5c) while

a single concordant analysis with a $^{207}\text{Pb}/^{206}\text{Pb}$ age of 3698 \pm 25 Ma was obtained for sample MB-GB-23A (Fig. 5b).

The trondhjemitic gneiss (TBE-19b) from the Borborema Province yields $^{207}\text{Pb}/^{206}\text{Pb}$ dates ranging from 3.59 to 3.53 Ga (Table S1). Concordant to slightly discordant analyses, from -1~% to 2~% (Table S1), define a regression line with upper intercept at 3577 \pm 11 Ma (n = 15, MSWD = 2.0) and lower intercept towards $\sim\!2.1~\text{Ga}$ (Fig. 5d). Two concordant analyses define a younger component with a $^{207}\text{Pb}/^{206}\text{Pb}$ WMA of 3487 \pm 14 Ma (Fig. 5d).

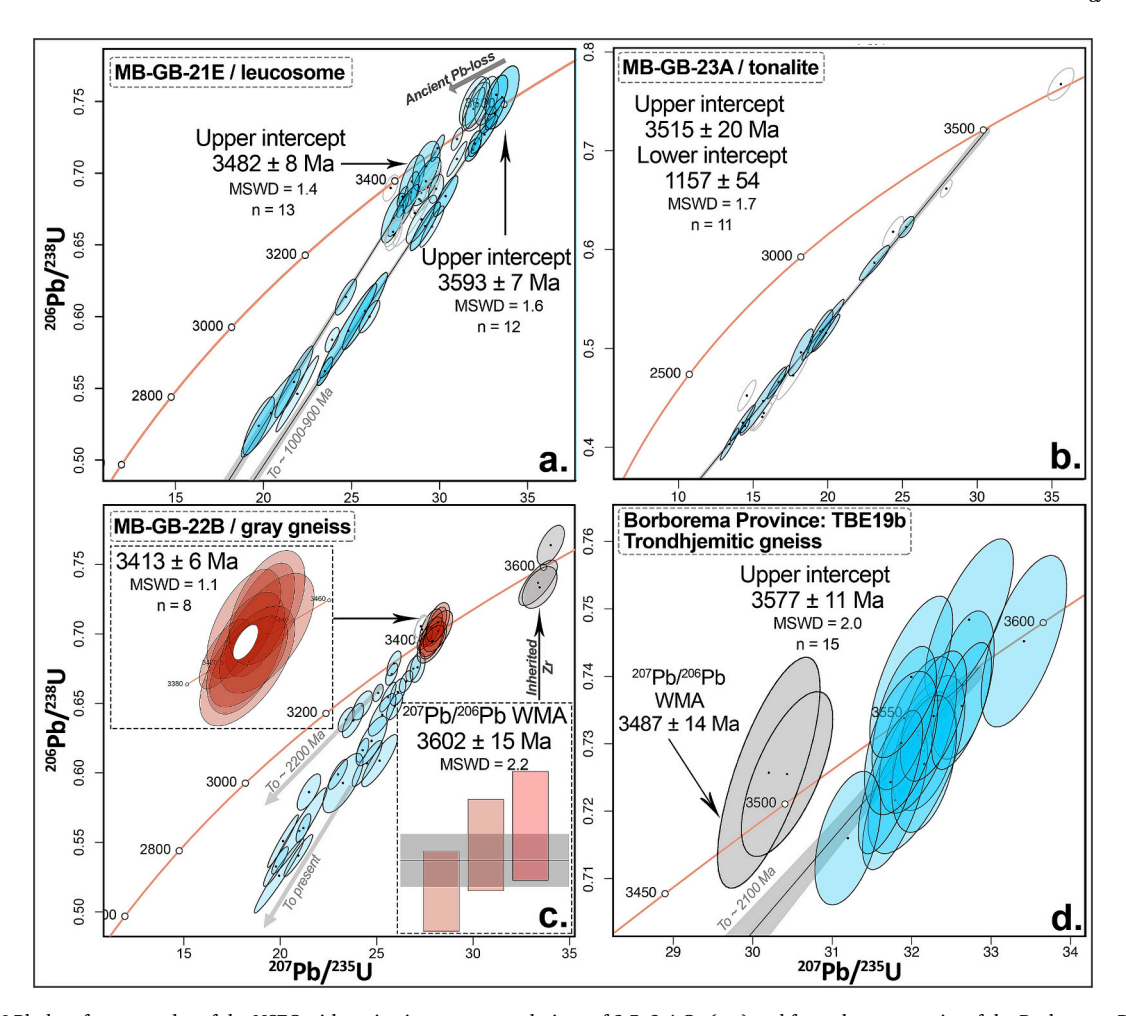


Fig. 5. Zircon U-Pb data from samples of the NSFC with main zircon age populations of 3.5–3.4 Ga (a-c) and from the gray gneiss of the Borborema Province (d). (a) MB-GB-21E, (b) MB-GB-23A, (c) MB-GB-22B, and (d) TBE-19b.

4.3. Zircon Lu-Hf isotopic results

Zircon Lu-Hf isotope compositions were determined from all samples analyzed for U-Pb (Figs. 6 and 7, Tables 1 and S2). The 3.61–3.59 Ga age cluster defined through zircon U-Pb in samples from the NSFC, define a narrow range of sub-chondritic initial Hf isotope compositions with weighted mean initial ϵ_{Hf} between -1.9 and -3.1 (Figs. 6 and 7, and Tables 1 and S2). The younger age cluster, with U-Pb ages between 3.52 and 3.41 Ga, yields chondritic to sub-chondritic initial Hf isotope compositions with mean initial ϵ_{Hf} between +0.7 and -3.2 (Figs. 6 and 7, Tables 1 and S2).

The initial Hf isotope compositions of samples with single age components are homogeneous within each sample with invariant 176 Hf/ 177 Hf plotted at their measured 207 Pb/ 206 Pb dates (Figs. 6 and 7). When calculating initial Hf isotope compositions at the best age determined for each of these samples, the 2-standard deviation (2 SD) is below 2 epsilon units, indicating single Hf isotope populations (Figs. 6 and 7). Complexities evidenced in the U-Pb data, with either concordant analyses plotting from \sim 3.6 to 3.5 Ga as in gray gneisses MB-GB-21C and MB-GB-21F (Figs. 4d-e) and the residue rich phase MB-GB-21B (Fig. 4a) or variably discordant analyses plotting along Discordia lines as in samples of the MB-GB-23 outcrop (Figs. 4f and 5b), are not reflected as heterogeneity in the Hf isotope data (Figs. 6 and 7).

Samples with two age clusters yield Hf isotope compositions consistent with distinct age and isotope components. Initial 176 Hf/ 177 Hf of zircon defining the old age component are lower than isotope ratios of grains within the younger age components (Figs. 6 and 7). Initial

 $^{176} \rm Hf/^{177} Hf$ isotopes are homogeneous within each age component with sub-horizontal trends through the $^{207} \rm Pb/^{206} Pb$ dates range. One example of this is the massive granitoid MB-GB-21A with age components of 3.59 and 3.52 Ga and mean initial Hf isotope compositions of $\epsilon_{\rm Hf(i)}$ –1.9 \pm 1.6 and +0.2 \pm 1.0 at 3.59 Ga and 3.52 Ga respectively (Fig. 6f). Similarly, inherited zircon yield Hf isotope compositions that differ from the isotope compositions of the main zircon population. Inherited zircon yield lower initial $^{176} \rm Hf/^{177} Hf$ isotope ratios that correspond to chondritic to sub-chondritic mean $\epsilon_{\rm Hf(3.7Ga)}$ of –0.5 \pm 0.8 (MB-GB-23A; Fig. 7b) and $\epsilon_{\rm Hf(3.6Ga)}$ of –2.6 \pm 0.8 (MB-GB-22B; Fig. 7c).

The trondhjemitic gneiss from the Borborema Province yields initial Hf isotope compositions around CHUR with $\epsilon_{Hf(3.6Ga)}$ from +1.2 to -1.6 (Table S2) and a weighted mean initial $\epsilon_{Hf(3.6Ga)}$ of -0.5 ± 1.5 (Fig. 7d). The 176 Hf/ 177 Hf isotope composition of this sample is homogeneous through the measured 207 Pb/ 206 Pb age range (3.59 to 3.54 Ga; Fig. 7d), indicating a homogeneous population.

5. Discussion

5.1. Bulk-rock petrogenesis

The analyzed samples from northeastern Brazil consist of migmatitic complexes, predominantly metatexites preserving gneissic structures, characterized by highly deformed fabrics. The whole-rock geochemistry from different components of migmatitic complexes are compositionally heterogeneous even within single outcrops with large ranges in concentrations of SiO₂, Al₂O₃, CaO, and ferromagnesian oxides (Table S3).

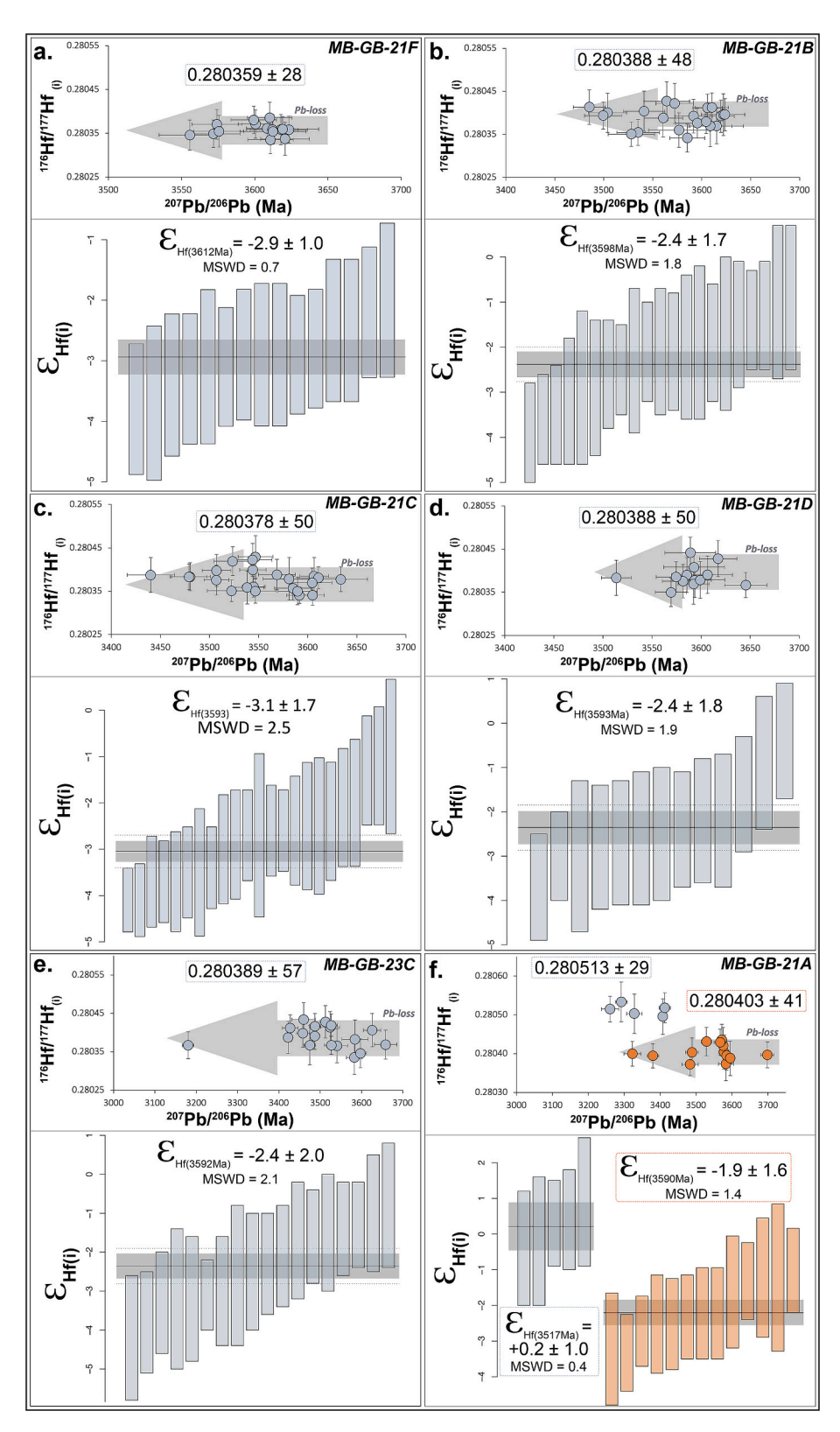


Fig. 6. Zircon Lu-Hf isotope data from samples from the NSFC with main 3.6 Ga components. (a) MB-GB-21F, (b) MB-GB-21B, (c) MB-GB-21C, (d) MB-GB21D, (e) MB-GB-23C, and (f) MB-GB-21A. Initial 176 Hf/ 177 Hf vs individual 207 Pb/ 206 Pb dates (top panels) and mean initial ϵ_{Hf} with 2 SD at crystallization age (bottom panels) are shown for each sample. Error bars of individual analysis are 2 SE for 176 Hf/ 177 Hf(i) and 207 Pb/ 206 Pb dates.

In the compositional ternary diagram of Laurent et al. (2014) most samples plot within the TTG field with three samples with higher concentrations of CaO, including residue rich phases, plotting in the field of hybrid granites (Fig. S8). The main component in these NSFC migmatitic

complexes are gray gneisses of calc-alkaline composition. Some rock phases such as the massive tonalite MB-GB-23A and three banded gneisses (MB-GB-21D, MB-GB-22B, and MB-GB-23C) share major (e.g., $\rm K_2O/Na2O<0.5$ at high $\rm SiO_2>65$ %) and trace element (e.g., low to

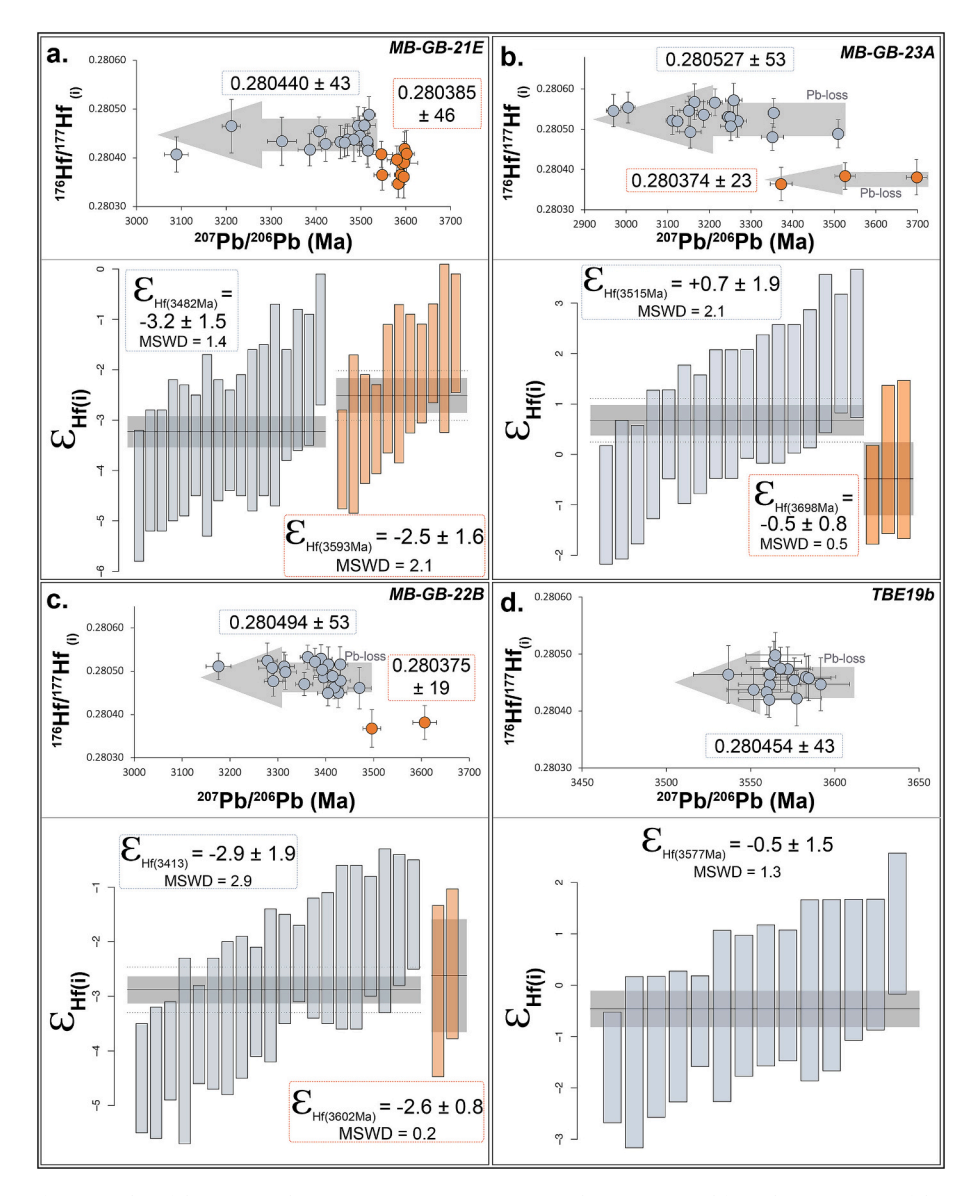


Fig. 7. Zircon Lu-Hf isotope from samples of the NSFC with main 3.5–3.4 Ga zircon age populations (a-c) and from the gray gneiss of the Borborema Province (d). (a) MB-GB-21E, (b) MB-GB-23A, (c) MB-GB-22B, and (d) TBE-19b. Initial 176 Hf/ 177 Hf vs individual 207 Pb/ 206 Pb age (top panels) and mean initial $\epsilon_{\rm Hf}$ with 2 SD at crystallization age (bottom panels) are shown for each sample. Error bars of individual analysis are 2 SE for 176 Hf/ 177 Hf_(i) and 207 Pb/ 206 Pb dates.

intermediate Sr and Y and high Nb concentrations) compositions with low to medium pressure TTGs as described by Moyen (2011) (Fig. S9). The major element chemistry of different rock phases is consistent with derivation from mafic sources with low to moderate K2O (Fig. S8). Tonalitic melts derived from the partial melting of a mafic source are consistent with TTG-like components within the Eo-Paleoarchean gneisses of the NSFC. Absent to weak negative Eu anomalies, observed in most rock phases, indicate that the melting of sources occurred at different crustal levels out of the stability of plagioclase (e.g., medium pressure TTGs) and at shallower depths (e.g., low pressure TTGs) within the stability of plagioclase (Moyen, 2011). The geochemical diversity of the migmatitic gneisses in the NSFC indicates either derivation from different sources or distinct fractionation processes during the genesis of these rocks. The geochronological data obtained from different geochemical components emphasize the complexity of the geological history recorded in these rocks.

5.2. U-Pb geochronology of Eo-Paleoarchean remnants from the northeastern Brazil

5.2.1. Zircon U-Pb geochronology of the northern São Francisco Craton (NSFC)

The oldest components determined in this study include inherited zircon with ²⁰⁷Pb/ ²⁰⁶Pb dates of 3.7 Ga and a main Eo-Paleoarchean age group with zircon U-Pb dates between 3.61 and 3.59 Ga (Fig. 8). Younger components with zircon U-Pb dates between 3.52 and 3.41 Ga are identified in four samples (MB-GB-21A, MB-GB-21E, MB-GB-23A, and MB-GB-23C) (Fig. 8). The main population of Eo-Paleoarchean zircon U-Pb ages between 3.61 and 3.59 Ga, determined for migmatitic gneisses in this study, are slightly younger than the oldest crystallization ages between 3.64 and 3.63 Ga that have been reported for orthogneisses within the Gavião Block (e.g., Moreira et al., 2022; Oliveira et al., 2020). The 3.64–3.63 Ga ages from previous studies were obtained from concordant to slightly discordant zircon analyses defining either Concordia ages or upper intercepts with MSWD around 1. Single zircon ²⁰⁷Pb/²⁰⁶Pb dates around ~3.63 Ga are commonly found in samples analyzed in this study (Table S1). The slightly younger ages

Chemical Geology 678 (2025) 122646

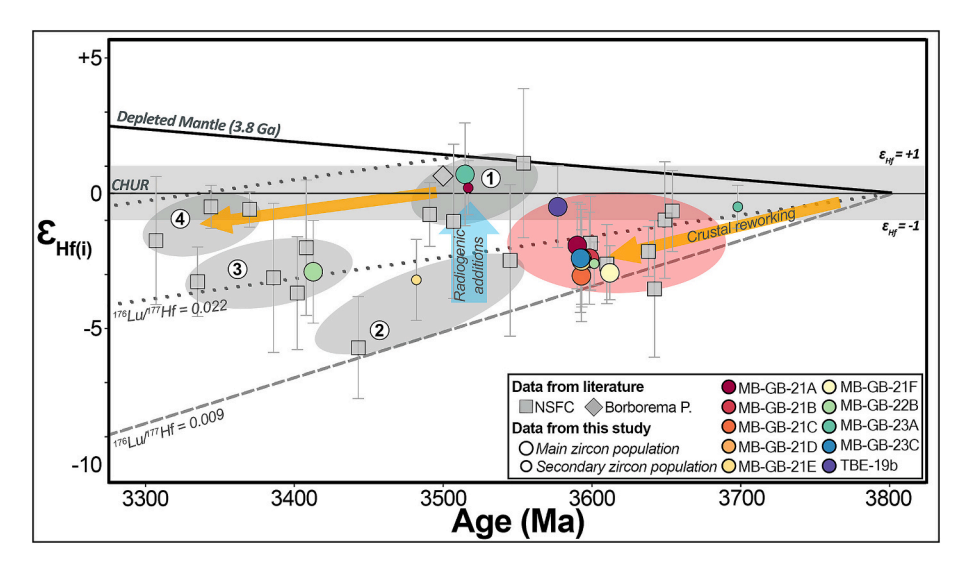


Fig. 8. Hf isotope data from samples in this study and the literature. Hf isotope data for each sample are plotted as mean epsilon Hf values with a 2 SD error bar. The main crustal forming event at \sim 3.65–3.60 Ga is highlighted with red-shaded oval. Isotope components between 3.5 and 3.3 Ga are numbered and highlighted with gray-shaded areas following the discussion presented in the main text. Hf schematic trajectories of 3.8 Ga mafic- (176 Lu/ 177 Hf \sim 0.022, Amelin et al., 1999) and TTG-like (176 Lu/ 177 Hf \sim 0.009, Gardiner et al., 2018) reservoirs are shown for reference. Data from the literature for the NSFC are from Moreira et al., 2022; Martins de Sousa et al., 2020; Oliveira et al., 2020; Santos-Pinto et al., 2012. Data from the Borborema Province are from Fachetti et al., 2024. (For interpretation of the references to color in this figure legend, the reader is referred to the web version of this article.)

used in this study as preferred crystallization ages result from calculating Concordia and/or weighted mean ²⁰⁷Pb/²⁰⁶Pb ages from consistent zircon age clusters, with at least 5 overlapping analyses, as reported in the results section. The U-Pb ages defining these age clusters, were determined on inner zircon domains (i.e., not from rims or overgrowths) with diverse textures in CL-images (e.g., homogeneous, patchy and sector zoning, and convoluted). Therefore, the Eoarchean-early Paleoarchean age components obtained in this study (3.61 and 3.59 Ga) are interpreted as primary crystallization ages for igneous protoliths of migmatitic gneiss complexes of the Gavião Block in concordance with previous studies. Together, the 3.64-3.59 Ga ages reported here and in previous studies define an initial time of crustal formation within the São Francisco Craton as previously suggested (e.g., dos Santos et al., 2022; Moreira et al., 2022; Nutman and Cordani, 1993; Oliveira et al., 2020; Paquette et al., 2015). Similar ages have not been reported for any other block within the craton suggesting that this Eo-Paleoarchean crust in the Gavião Block is the oldest stable crust preserved in the craton, and likely served as an old core from which the craton further grew.

The 3.64-3.59 Ga main crustal forming event in the Gavião Block was followed by renewed magmatism between 3.52 and 3.41 Ga recorded by zircon U-Pb in this study. During this time, rocks experienced anatexis, as supported by the 3.48 Ga component in leucosome MB-GB-21E, and (re)crystallization of new zircon and zircon domains defining 3.52–3.41 Ga age populations in gneisses and granitoids in this study (Figs. 4 and 5). This high-temperature event is reflected as ancient Pb-loss in the ~3.6 Ga rocks with concordant zircon analyses plotting along the Concordia from ~3.63 to ~3.48 Ga (Figs. 4 and 5). Magmatism between 3.5 and 3.3 Ga, often accompanied by migmatization, is widely recorded within the Gavião Block (e.g., Lopes et al., 2021; Martins de Sousa et al., 2020; Moreira et al., 2022; Zincone et al., 2016) and to a lesser extent in other areas of the northern São Francisco Craton (e.g., Barbosa et al., 2020). Furthermore, a longer thermal perturbation is suggested by zircon domains, described as metamorphic in origin, with reported U-Pb ages between ~3.4 and ~3.2 Ga in orthogneisses within the Gavião Block (e.g., Moreira et al., 2022).

Older crustal components have been inferred by inheritance in granodioritic gneisses in the Gavião Block with relict zircon with $^{207}\text{Pb}/^{206}\text{Pb}$ ages between 3.70 and 3.67 Ga (Moreira et al., 2022; Oliveira et al., 2020). Two single zircon grains with $^{207}\text{Pb}/^{206}\text{Pb}$ ages of

 3698 ± 25 Ma (1 % discordant) and 3698 ± 18 Ma (3 % discordant) were determined for the tonalite MB-GB-23A and massive granitoid MB-GB-21A, respectively (Table S1). Hadean to Eoarchean single zircon dates reported from a supracrustal sequence (²⁰⁷Pb/²⁰⁶Pb age of 4.1 Ga; Paquette et al., 2015), and from an orthogneiss (207Pb/206Pb age of 3.8 Ga; Guitreau et al., 2012) have been used to argue for the existence of Hadean to Eoarchean crust in the northern São Francisco Craton. The Hadean age reported in Paquette et al. (2015), was obtained from 16 individual spots performed on a single zircon, interpreted as igneous in origin, with variable discordance between 2 % and 24 % defining a Discordia line with an upper intercept at 4096 \pm 23 Ma. The 3.8 Ga zircon reported in Guitreau et al. (2012) is highly discordant (54 % discordant); accordingly, we do not consider this zircon date sufficiently reliable to make inferences on the existence of Hadean-early Eoarchean crust within the São Francisco Craton. Concordant to slightly discordant inherited zircon within the Gavião Block reported in this and previous studies (i.e., Moreira et al., 2022; Oliveira et al., 2020), with ²⁰⁷Pb/²⁰⁶Pb ages between 3.70 and 3.67 Ga, provide more robust evidence for preexisting evolved crust in the São Francisco Craton that either did not survive as a coherent crustal block or that simply has not yet been found. Suggestions of an older crustal component (i.e., Hadean) within the craton based on a single Hadean zircon is speculative.

5.2.2. Zircon U-Pb geochronology of the Borborema Province

In this study we also dated a trondhjemitic gneiss from the Borborema Province. Concordant to slightly discordant zircon analyses with $^{207}\text{Pb}/^{206}\text{Pb}$ dates between 3.59 and 3.55 Ga plot along a regression line and define an upper-intercept age of 3.58 Ga for this trondhjemite (Fig. 5d). A younger component is defined by two overlapping concordant zircon analyses at 3.48 Ga (Fig. 5d).

Paleoarchean zircon U-Pb ages reported for TTG gneisses in the Borborema Province are dominantly 3.4 to 3.3 Ga (e.g., Dantas et al., 2013; Dantas et al., 2004; Fachetti et al., 2024; Neves, 2021; Pitarello et al., 2019). Older components, scarcer in the literature, include TTGs and meta-mafic rocks with zircon U-Pb ages ranging from 3.55 to 3.51 Ga (e.g., Pitarello et al., 2019; Santos et al., 2020) and one serpentinite in the northern part of the province with an Eoarchean age of 3.7 Ga (Santos et al., 2020). Trondhjemitic and granodioritic gneisses, from the same outcrop as the gneiss analyzed in this study, have reported zircon

ages of 3.58 and 3.47 Ga, respectively (Neves et al., 2022) in concordance with the age reported in this study for the trondhjemitic phase (Fig. 5d). Meso- to Neoarchean components are abundant in the Borborema Province with main age clusters at 3.1–3.0 Ga and ~2.9-2.6 Ga (e.g., Neves et al., 2022; Fachetti et al., 2024; Ferreira et al., 2020; Pitarello et al., 2019).

Data from this study confirm presence of a ~3.6 Ga component within the Borborema Province previously identified for the trondhjemitic phase (Neves et al., 2022). The younger 3.48 Ga component in a trondhjemitic phase is consistent with the 3.47 Ga age reported for a granodioritic gneiss within the same TTG sequence (Neves et al., 2022). Several magmatic pulses between 3.4 and 2.7 Ga, in most cases accompanied with migmatization and metamorphism, are recorded locally in TTG enclaves in the central and northern parts of the Borborema Province (e.g., da Silva Filho et al., 2002; Dantas et al., 2013; Dantas et al., 2004; Fachetti et al., 2024; Ferreira et al., 2020; Neves et al., 2022; Pitarello et al., 2019).

Magmatic components identified in the Borborema Province at ~ 3.6 Ga, ~3.5 Ga, and 3.4-3.3 Ga (e.g., this study; Neves et al., 2022; Dantas et al., 2004, 2013; Fachetti et al., 2024; Pitarello et al., 2019) are comparable with periods of crustal formation at $\sim 3.65-3.60$ Ga, \sim 3.52–3.48 Ga, and 3.4–3.3 Ga in the northern São Francisco Craton (e. g., this study; Moreira et al., 2022; Guitreau et al., 2012; Lopes et al., 2021; Martins de Sousa et al., 2020; Oliveira et al., 2020; Zincone et al., 2016). Similar records of Meso- and Neoarchean magmatism in both the Gavião Block and the Borborema Province have been discussed before (e.g., Ganade et al., 2021) and led to the suggestion of a Neoarchean Gavião-Campestre nucleus (Neves, 2021). The fact that a TTG gneiss enclave from the Borborema Province records a ~3.6 Ga age, only identified in the Gavião Block within the craton, along with comparable 3.5-3.3 Ga magmatic histories in both terrains, suggest a shared crustal evolution from the Paleoarchean through at least the Neoarchean. Disaggregation and displacement of ancient crustal fragments, including those within the Borborema Province, along with deformation are suggested to have occurred during Early Neoproterozoic rifting-driven decratonization followed by orogenic reworking (Ganade et al., 2021).

5.3. Hf isotope evolution of Eo-Paleoarchean crust in northeastern Brazil

5.3.1. Northern São Francisco Craton

Eo-Paleoarchean components of migmatitic gneisses from this study yield consistently chondritic to sub-chondritic initial Hf isotope compositions ranging from $\epsilon_{Hf(i)}$ +0.7 to -3.2 (Fig. 8). Initial Hf isotope compositions calculated for the 3.61-3.59 Ga components are within error of each other with $\xi_{Hf(i)}$ between -1.9 and -3.1 (Fig. 8). Renewed magmatism between 3.52 and 3.41 Ga yields chondritic to subchondritic Hf isotope compositions with initial $\boldsymbol{\xi}_{Hf}$ between +0.2 and -3.2 (Fig. 8). Inherited zircon yield individual initial ξ_{Hf} of $+0.5\pm1.2$ and -1.5 ± 1.4 at ~ 3.7 Ga (Table S2) consistent with the chondritic ξ_{Hf} $_{(3.7Ga)}$ of -0.5 ± 0.8 determined from three zircon grains in the tonalite (MB-GB-23A) with overlapping initial ¹⁷⁶Hf/¹⁷⁷Hf at individual ²⁰⁷Pb/²⁰⁶Pb ages (Fig. 7b). The relatively homogenous Hf isotope compositions of samples with main age component around 3.6 Ga, despite showing complexities in the U-Pb system-such as in the diorite (MB-GB-21B; Fig. 4a) and the gray gneiss MB-GB-21C (Fig. 4e), which exhibit ancient and recent Pb-loss trends-support the interpretation that the ~3.6 Ga component represents the most reliable estimate for crystallization ages of these rocks.

Isotope compositions with initial E_{Hf} between -1.5 and -3.0 have been reported for 3.65–3.60 Ga orthogenesis within the Gavião Block (e. g., Moreira et al., 2022; Oliveira et al., 2020). Younger components associated with magmatism and migmatization between 3.55 and 3.30 Ga have reported more variable initial Hf isotope compositions with E_{Hf} (i) between +2.4 to -9.0 (e.g., dos Santos et al., 2022; Guitreau et al., 2012; Martins de Sousa et al., 2020; Moreira et al., 2022; Santos-Pinto et al., 2012) The Hf isotope compositions reported for some of the

~3.65–3.60 Ga gneisses in previous studies show large dispersions in initial ξ_{Hf} with 2 SD over 3 epsilon units (e.g., $\xi_{Hf(3.64Ga)}$ -3.0 \pm 3.8 from Oliveira et al., 2020). Similarly, variations in initial Hf isotope compositions in ~3.5-3.3 Ga gneisses calculated at assigned crystallization age are over 3 epsilon units (2 SD) in some samples reported in de Moreira et al. (2022), dos Santos et al. (2022), and Guitreau et al. (2012). Additionally, individual analyses with high in-run uncertainties (e.g., 2 SE of 3 to 7 epsilon Hf units) are reported for some samples in dos Santos et al. (2022) and Guitreau et al. (2012). The isotopic variability in the Hf isotope data reported for Eo-Paleoarchean gneisses in previous studies can reflect mixing of different components and/or high in-run uncertainties. Metamorphic domains and xenocryst cores are described in previous studies. Mixing of different domains within zircon grains during analysis resulting in isotope heterogeneity, therefore, is highly plausible. If the latter is the case, the Hf isotope composition of even a "good" analysis with low in-run uncertainty (i.e., 2 SE < 2 epsilon units) may not reflect the primary magmatic Hf isotope composition. Additionally, positive correlations between ¹⁷⁶Hf/¹⁷⁷Hf and ¹⁷⁶Yb/¹⁷⁷Hf ratios as evidenced in data from de Moreira et al. (2022), suggest under correction of ¹⁷⁶Yb interference resulting in higher ¹⁷⁶Hf/¹⁷⁷Hf ratios relative to a true value (e.g., Fisher et al., 2014) that will lead to inaccurate calculation of initial Hf isotope compositions.

After filtering the available Hf isotope data, that involve exclusion of analyses with high in-run errors (2 SE < 2 ϵ units) and samples with variations of 2 SD over 3 epsilon units, reported in previous studies for the Gavião block (Guitreau et al., 2012; Martins de Sousa et al., 2020; Moreira et al., 2022; Oliveira et al., 2020; Santos-Pinto et al., 2012) the initial Hf isotope compositions for the 3.65-3.60 Ga gneisses range from $\xi_{\rm Hf(i)}$ -1.5 to -3.5 (Fig. 11). This refined range in the Hf isotope compositions for 3.65-3.60 Ga gneisses is identical within error with Hf isotope compositions determined here for the ~3.6 Ga orthogneisses between $\xi_{Hf(3.6Ga)}$ -1.9 to -3.1 (shaded red area in Fig. 8). The Hf isotope data for the 3.55-3.31 Ga gneisses and granitoids can be roughly separated into 4 groups (Fig. 8): 1) radiogenic Hf isotope compositions with $\xi_{Hf(i)}$ from +1.1 to -1.0 between 3.55 and 3.49 Ga; 2) subchondritic values, with progressively more negative ξ_{Hf} values over time, from $\xi_{Hf(i)}$ -2.5 at ~3.55 Ga to $\xi_{Hf(i)}$ -5.7 at 3.44 Ga; 3) more radiogenic isotope compositions with $\xi_{Hf(i)}$ between -2.0 and -3.7 at \sim 3.41–3.35 Ga; and 4) slightly sub-chondritic $\epsilon_{Hf(i)}$ from -0.5 to -1.7at \sim 3.4–3.3 Ga. Isotope compositions determined for the \sim 3.52 Ga components, ($\xi_{Hf(i)}$ of +0.7 and +0.2), and for the ${\sim}3.49{\text{--}}3.41$ Ga components ($\xi_{Hf(i)}$ of -2.9 and -3.2) are in good agreement with the filtered isotope data from rocks of similar ages within the Gavião Block (Fig. 8).

Together, the Hf isotope data reported here, and in previous studies for Eo-Paleoarchean gneisses in the northern São Francisco Craton, are consistently sub-chondritic ($\xi_{Hf(\sim 3.6Ga)}$ from -1.5 to -3.5) for the 3.65-3.59 Ga main crustal forming event and more variable for later magmatic events between 3.55 and 3.30 Ga ($\xi_{Hf(i)}$ between +1.1 to -5.7) (Fig. 8). A Hadean precursor for the 3.65-3.59 Ga gneisses has been proposed based on the assumption of derivation from a depleted mantle reservoir (e.g., dos Santos et al., 2022; Oliveira et al., 2020). Additionally, unradiogenic initial Hf isotope compositions determined for ${\sim}3.7$ Ga xenocrysts with negative $\xi_{Hf(i)}$ between -4.9 and -8.6 have been used to support the existence of a Hadean precursor and early mantle differentiation (e.g., dos Santos et al., 2022; Oliveira et al., 2020). Such unradiogenic compositions reflect reworking and assimilation of pre-existent Hadean crust without implying significant differentiation of the mantle to produce a depleted mantle source in the Hadean-early Eoarchean. Crustal reworking and assimilation alone without involvement of juvenile mantle-derived material have been, in fact, proposed for some of the oldest crustal components on Earth including the Eoarchean Acasta gneiss complex and gneisses from west Greenland, and Hadean Jack Hill zircons with chondritic to subchondritic Hf isotope compositions (e.g., Bauer et al., 2017; Fisher and Vervoort, 2018; Iizuka et al., 2009; Kemp et al., 2010). The subchondritic initial Hf isotope compositions and lack of evidence for juvenile mantle-derived sources for the genesis of the 3.65–3.60 Ga gneisses within the Gavião Block do not support derivation from a depleted mantle source.

We interpret the consistently sub-chondritic initial Hf isotope compositions reported here and previous studies (i.e., Moreira et al., 2022; Oliveira et al., 2020) for the ~3.6 Ga orthogneisses within the Gavião Block to indicate derivation from a reservoir of broadly chondritic isotope composition and/or reworking of a \sim 3.8 Ga pre-existing crust. This is also supported by Hf trajectories of mafic- ($^{176}Lu/^{177}$ Hf ~ 0.022 ; Amelin et al., 1999) and TTG-like (176Lu/177Hf ~0.009; Gardiner et al., 2018) reservoirs evolving from CHUR at 3.8 Ga to the Hf isotope compositions of ~3.6 Ga components of the NSFC (Fig. 8). An Eoarchean precursor of broadly chondritic isotope composition is in agreement with previous work within the Gavião Block (Moreira et al., 2022) and other 3.8-3.6 Ga gneisses worldwide (e.g., Amelin et al., 2011; Bauer et al., 2017; Fisher and Vervoort, 2018; Kemp et al., 2019; Mulder et al., 2021). Melting of a precursor of mafic composition, in agreement with models for generation of TTG melts in the Archean (e.g., Martin, 1993; Moven and Martin, 2012), is consistent with ~3.6 Ga components of TTG affinity within migmatitic complexes in the NSFC. Furthermore, interaction of melts generated at different depths through mingling and/ or mixing combined with different degrees of melting and fractional crystallization occurring on short-time scales could explain the compositional diversity observed in migmatitic gneisses in the NSFC, that contrast with their relatively homogeneous isotope compositions (e.g., Laurent et al., 2014).

Reworking of a ~3.6 Ga crust alone, with isotope composition similar to that of main ~ 3.6 Ga components of the NSFC ($\xi_{Hf(3.6Ga)} - 1.9$ to -3.1; Fig. 8), with either mafic-like 176 Lu/ 177 Hf ~ 0.022 or TTG-like $^{176}\text{Lu}/^{177}\text{Hf}\sim0.009$ would result in $\xi_{\text{Hf(i)}}$ from -2.7 to -4.8 and $\xi_{\text{Hf(i)}}$ between -3.5 and -6.5 at 3.5 Ga and 3.4 Ga, respectively. Even more unradiogenic values, $\xi_{Hf(3.5Ga)}$ between -4.1 and -5.3 Ga and $\xi_{Hf(3.4Ga)}$ between -6.3 and -7.5, result from the isotope evolution of zircon alone (e.g., recrystallization of zircon grains/domains) owing that epsilon Hf values in zircon change by about 2.2 epsilon units per 100 Ma. To produce the slightly super-chondritic initial Hf isotope composition at \sim 3.5 Ga ($\xi_{Hf(3.5Ga)}$ +0.7 and +0.2) and the less unradiogenic isotope composition determined at $\sim\!3.4$ Ga ($\xi_{Hf\,(3.4Ga)}\,{-}2.9$), a more radiogenic component must be involved. Incorporation of juvenile material has been invoked for the genesis of a 3.54 Ga gneiss within the Gavião Block with a slightly super-chondritic initial Hf isotope composition of $\mathcal{E}_{Hf(i)}$ of +1.1 (Fig. 8; Moreira et al., 2022). The radiogenic Hf isotope composition of the 3.52 Ga components ($\xi_{Hf(i)}$ of +0.7 and +0.2; Fig. 8) is consistent with renewed magmatism involving more juvenile isotope components and assimilation of ~3.6 Ga crust. Reworking of 3.6 and 3.5 Ga crustal components without significant transfer of radiogenic components during anatexis and late magmatism are indicated by the sub-chondritic isotope compositions of a leucosome ($\xi_{Hf(3.48Ga)}$ –3.2) and late magmatic component ($\xi_{Hf(3.4Ga)}$ -2.9) (Fig. 8). Similar Hf isotope patterns with crustal reworking signatures followed by inputs of more radiogenic Hf have been described in other Precambrian terranes including the Acasta gneiss complex and Yilgarn craton (e.g., Bauer et al., 2017; Kemp et al., 2010; Mulder et al., 2021). Isotope shifts towards more juvenile Hf isotope compositions have been interpreted to reflect changes in crust-forming mechanisms and geodynamic regimes that promote crustal stabilization (e.g., Mulder et al., 2021; Næraa et al., 2012), at least at a local scale (e.g., Kemp et al., 2023; Laurent et al., 2024).

5.3.2. The Borborema Province

A trondhjemitic gneiss analyzed here within the Borborema Province yields a slightly sub-chondritic Hf isotope composition with initial $\epsilon_{Hf(i)}$ of -0.5 ± 1.5 at 3.58 Ga. Homogeneous isotope composition is determined for this gneiss with initial $^{176}\text{Hf}/^{177}\text{Hf}$ at individual $^{207}\text{Pb}/^{206}\text{Pb}$ ages with a variation of 1.5 epsilon units (Fig. 7d).

Isotope data in the literature are scarce for Paleoarchean components within the Borborema Province. Fachetti et al. (2024) recently reported Hf isotope compositions for Paleoarchean components from migmatitic orthogneisses within the central part of the province that include 2 analyses of a single grain with $\epsilon_{Hf(i)}$ of $+0.8\pm1.0$ and $+0.5\pm1.5$ at 3.5 Ga, a single analysis with $\epsilon_{Hf(i)}-1.4\pm3.4$ at 3.4 Ga, and 3 analyses from 2 grains with $\epsilon_{Hf(i)}$ between -3.3 and -3.6 at 3.3 Ga. No Hf isotope data have been reported for $\sim\!3.6$ Ga components within the Borborema Province before this study.

Nearly chondritic initial Hf isotope compositions ($\xi_{Hf(3.6Ga)}$ of -0.5 \pm 1.5) obtained in this study, the first high-precision data reported for the \sim 3.6 Ga component within the Borborema Province, is consistent with derivation from a Eoarchean source of broadly chondritic composition. Furthermore, a chondritic reservoir is supported by Hf isotope data reported in this study (Fig. 7d) and in Fachetti et al. (2024) for the 3.6 and 3.5 Ga components, respectively. Sub-chondritic isotope compositions between $\xi_{Hf(3.3Ga)}$ –3.3 and –3.6 (Fachetti et al., 2024) of the ~3.3 Ga magmatism suggest reworking of the 3.6–3.5 Ga components with no significant addition of juvenile mantle-derived material. A main crustal forming event at ~3.6 Ga with sub-chondritic initial Hf isotope compositions ($\xi_{Hf(3.6Ga)}$ from -1.5 to -3.5; Fig. 8) followed by younger juvenile additions at $\sim 3.5-3.3$ Ga ($\xi_{Hf(3.6Ga)}$ from -1.5 to -3.5; Fig. 8) recorded in both the NSFC and the Borborema Province, support a shared crustal evolution during the Paleoarchean for these ancient remnants of northeastern Brazil.

5.4. Implications on the global Hf isotope record of the Primitive Earth

The Hf and Nd isotope records of Precambrian terranes have been pivotal in constraining models of crustal growth during Earth's early history. These are grouped in 2 end-member models: one proposes that present-day crustal volumes formed by 4 Ga with minimal subsequent growth (e.g., Armstrong, 1991; Bowring and Housh, 1995); the other suggests that crustal growth was progressive, with significant formation and preservation of continental crust only after ~3.8 Ga (e.g., McLennan and Taylor, 1982; Patchett and Arndt, 1986). Similarly, contrasting views exist on the formation of the depleted mantle reservoir suggesting either extensive development since the Hadean (e.g., Bennett et al., 1993; Bowring and Housh, 1995) or significant depletion beginning at ~3.8 Ga (e.g., Vervoort et al., 2013; Vervoort et al., 2012; Vervoort and Kemp, 2025; Vervoort and Kemp, 2016). Hf isotope records from welldated zircon in Eoarchean-Paleoarchean rocks, along with Hadean detrital zircon from the Jack Hills, reveal key observations (Fig. 9): 1) The oldest magmatic zircon from the Acasta gneiss complex and detrital zircon from the Jack Hills are sub-chondritic with increasingly negative E_{Hf(i)} for younger grains, indicating intra-crustal reworking without significant incorporation of radiogenic components; 2) The most radiogenic zircons follow a chondritic evolution through ~3.8 to ~3.6 Ga; 3) It is not until \sim 3.6 Ga that the most radiogenic zircon deviate above chondritic evolution. We take this as the beginning formation of a sustained-and long lasting-depleted mantle reservoir; 4) Throughout all of the Archean there is a trend towards more negative $\boldsymbol{\xi}_{Hf}$ values with increasingly younger samples, consistent with reworking of older crust. The global Hf isotope record highlights the near absence of Hadean crust and the increasing crustal abundance from the Eoarchean through the Paleoarchean, with gradual appearance of mixing trends involving a depleted mantle source and evolved crust. These observations support a model of progressive crustal growth and the late development of a depleted mantle reservoir.

Precambrian terrains such as Yilgarn, Wyoming, and Slave exhibit shifts from sub-chondritic to more radiogenic Hf isotope compositions (e.g., Bauer et al., 2017; Frost et al., 2017; Kemp et al., 2010; Mulder et al., 2021). Although there are too few data to say anything definitive for the NSFC, there is a hint of a shift in the Hf isotope record at around ~3.5 Ga consistent with this trend (Fig. 8). These shifts, potentially indicating a transition from intra-crustal reworking to crustal

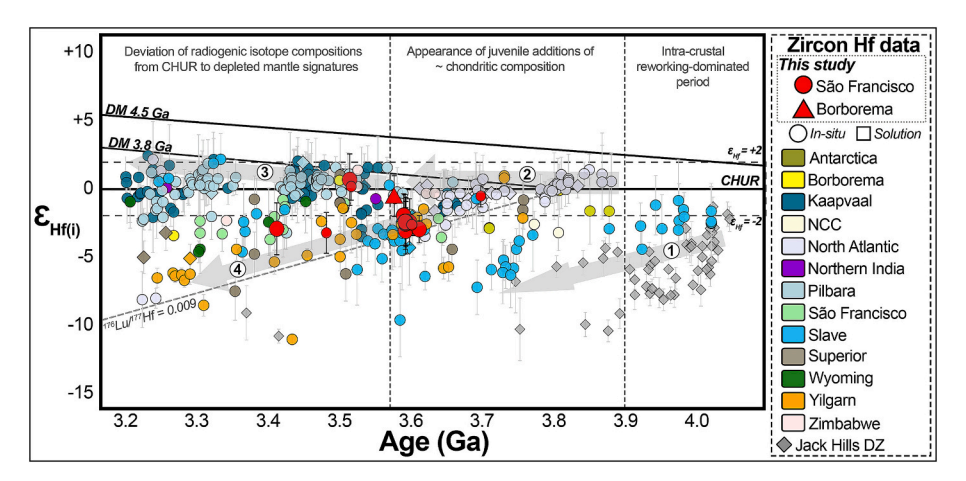


Fig. 9. Hf isotope data compilation from Precambrian terranes modified after Vervoort and Kemp, 2025. Hf schematic trajectory of a TTG-like reservoir is shown for reference (176 Lu/ 177 Hf \sim 0.009, Gardiner et al., 2018). Numbers and arrows are shown to highlight features that are discussed in the main text. References used in this plot are listed in supplementary materials.

rejuvenation, have been interpreted to reflect changes in crust-forming mechanisms and geodynamics that promoted crustal stabilization (e. g., Mulder et al., 2021). Isotopic shifts, however, are not recorded in all Precambrian terranes. Individual Archean cratons display different patterns in their Hf isotope records, with juvenile additions and depleted mantle signatures appearing diachronously (Fig. 9). These variations suggest that changes in geodynamics and crust-forming processes occurred at regional scales, driven by local mantle and crustal components and varying rates of crustal formation, rather than synchronous global changes or the onset of convergent tectonics (e.g., Kemp et al., 2023; Laurent et al., 2024).

An important remaining question is how the Hf isotope record correlates with the Nd isotope record in ancient rocks from Brazil as well as worldwide. The Nd isotope records show much greater isotope heterogeneity (Vervoort and Kemp, 2025) which has been interpreted to indicate extensive extraction of crust and development of a depleted mantle source in the Hadean-Eoarchean (e.g., Bennett et al., 1993; Bowring and Housh, 1995; Hoffmann et al., 2011; Hoffmann et al., 2010). These data, however, largely from bulk-rock samples, may have been compromised by the mixing of different components in the analyzed sample and by open-system behavior due to postcrystallization thermal perturbations (e.g., Vervoort and Kemp, 2025). Such disturbances have been illustrated by REE-rich mineral phases from Eo-Paleoarchean rocks from west Greenland and Acasta gneiss complexes which indicate Sm-Nd re-equilibration in the Neoarchean and Paleoproterozoic (e.g., Fisher et al., 2020; Hammerli et al., 2019; Kemp et al., 2019). Additionally, the coexistence of components with distinct ages and isotope compositions within individual samples, as demonstrated for Eo-Paleoarchean gneisses in the São Francisco Craton (this study), as well as from west Greenland, Acasta, and Minnesota River valley (e.g., Fisher et al., 2020; Hammerli et al., 2019; Kemp et al., 2019; Wang et al., 2020), further indicate isotope complexities at the bulk-rock scale. We suggest that Hf isotope compositions determined on well-dated zircon samples provide a more reliable isotope record of the primitive Earth, especially in complex polymetamorphic terrains such as in northeastern Brazil. The zircon Hf isotope record, as shown here in northeast Brazil as well as worldwide, suggests extensive development of the depleted mantle and the appearance of evolved crust later in the Paleoarchean, coinciding with the appearance of continental crust in the geologic record.

5.5. Concluding remarks

Eo-Paleoarchean components of northeastern Brazil record a main crust forming period at \sim 3.6 Ga followed by renewed magmatism and

anatexis between 3.5 and 3.4 Ga. The 3.65–3.60 Ga gneisses of the northern São Francisco Craton yield sub-chondritic Hf isotope compositions consistent with derivation from melting of a \sim 3.8 Ga mafic source of broadly chondritic composition. Late magmatism at \sim 3.52 and 3.41 Ga following the main \sim 3.6 Ga crustal forming episode, with slightly supra-chondritic to sub-chondritic initial Hf isotope compositions, suggests crustal reworking of the 3.65–3.60 Ga crust along with inputs of a more radiogenic component. A similar Hf isotope record is observed in the Borborema Province with a main \sim 3.6 Ga age component with slightly sub-chondritic (EHf(3.6Ga) of -1) isotope composition followed by a younger juvenile addition at \sim 3.5 Ga with EHf(i) of +1 (Fig. 8). Comparable geochronological and Hf isotopic records of EoPaleoarchean rocks from the northern São Francisco Craton and the Borborema Province suggest a shared crustal evolution from the Paleoarchean through at least the Neoarchean.

The Hf isotope record of well-known Precambrian terranes worldwide indicates that intra-crustal reworking prevailed through the Hadean and early Eoarchean, while juvenile additions of chondritic isotope composition appear after ~3.8 Ga (Fig. 9). Prominent depleted mantle signatures only emerge after ~3.5 Ga. The Hf isotope record reported here for Eo-Paleoarchean rocks of northeastern Brazil follows that of the global zircon Hf isotope record. Poly-metamorphic rocks characteristic of Precambrian terranes often record multiple post-crystallization thermal perturbations and have distinct age and isotope components, leading to isotope complexities at the bulk-rock scale. In complex, multicomponent rocks such Archean migmatitic gneisses, in-situ Hf isotope compositions of magmatic zircon grains/domains provide the most reliable isotope record for clarifying the evolution of the crust-mantle system in the early Earth. This Hf isotope record is consistent with the existence of a mantle reservoir of broadly chondritic isotope composition through the Hadean-Eoarchean, with a sustained depleted mantle reservoir only forming later in the Paleoarchean.

CRediT authorship contribution statement

Manuela Botero: Writing – review & editing, Writing – original draft, Visualization, Methodology, Investigation, Funding acquisition, Formal analysis, Conceptualization. Jeffrey D. Vervoort: Writing – review & editing, Supervision, Methodology, Funding acquisition, Conceptualization, Formal analysis. Vinicius T. Meira: Writing – review & editing, Conceptualization. Daniel F. Martins de Sousa: Writing – review & editing. Ticiano J.S. Santos: Writing – review & editing.

Declaration of competing interest

The authors declare that they have no known competing financial interests or personal relationships that could have appeared to influence the work reported in this paper.

Data availability

All data is included in supplementary materials

Acknowledgements

We thank Dr. Victor Valencia at Washington State University and Zirchron for his support in sample preparation, mineral separation, and U-Pb analytical procedures. We also thank Charles Knaack and Peter Baker at the Radiogenic Isotope and Geochronology Laboratory (RIGL) at Washington State University for technical support in inductively coupled plasma-mass spectrometry and the cleaning lab. This project was supported with funding from the National Science Foundation grants EAR-2222254 to Jeffrey Vervoort. Botero thanks Fulbright Colombia for the funds to support her doctoral studies at Washington State University (Fulbright-Minciencias award - cohort 2020) and the Geological Society of America for the funds provided through the GSA Graduate Student Research Grant 2022 (13723-22) to support field work in Brazil. Meira and Santos acknowledge National Council for Scientific and Technological Development (CNPq) for productivity fellowship process 314473/2021-1 and 310860/2022-9, respectively. The paper benefited from constructive reviews by Oscar Laurent and Jack Mulder and the editorial handling by Sonja Aulbach.

Appendix A. Supplementary data

Supplementary data to this article can be found online at https://doi.org/10.1016/j.chemgeo.2025.122646.

References

- Amelin, Y., Lee, D.C., Halliday, A.N., 2000. Early-middle Archaean crustal evolution deduced from Lu-Hf and U-Pb isotopic studies of single zircon grains. Geochimica et Cosmochimica Acta 64 (24), 4205–4225.
- Amelin, Y., Lee, D.C., Halliday, A.N., Pidgeon, R.T., 1999. Nature of the Earth's earliest crust from hafnium isotopes in single detrital zircons. Nature 399, 252–255. https:// doi.org/10.1038/20426
- Amelin, Y., Kamo, S.L., Lee, D.C., 2011. Evolution of early crust in chondritic or nonchondritic Earth inferred from U-Pb and Lu-Hf data for chemically abraded zircon from the Itsaq Gneiss complex, West Greenland. Can. J. Earth Sci. 48, 141–160. https://doi.org/10.1139/E10-091.
- Armstrong, R.L., 1991. The persistent myth of crustal growth. Aust. J. Earth Sci. 38, 613–630. https://doi.org/10.1080/08120099108727995.
- Barbosa, J.S.F., Barbosa, R.G., 2017. The Paleoproterozoic Eastern Bahia Orogenic Domain. In: Heilbron, M., Cordani, U.G., Alkmim, F.F. (Eds.), S\u00e3o Francisco Craton, Eastern Brazil: Tectonic Genealogy of a Miniature Continent. Springer International Publishing, Cham, pp. 57–69. https://doi.org/10.1007/978-3-319-01715-0_4.
- Barbosa, N.S., Menezes Leal, A.B., Debruyne, D., Bastos Leal, L.R., Marinho, M., Mercês, L., Barbosa, J.S.F., Koproski, L.M., 2020. Paleoarchean to Paleoproterozoic crustal evolution in the Guanambi-Correntina block (GCB), north São Francisco Craton, Brazil, unraveled by U-Pb Geochronology, Nd-Sr isotopes and geochemical constraints. Precambrian Res 340, 105614. https://doi.org/10.1016/j.precamres.2020.105614.
- Barbosa, J.S.F., Sabaté, P., 2004. Archean and Paleoproterozoic crust of the São Francisco Craton, Bahia, Brazil: Geodynamic features. Precambrian Res. 133, 1–27. https://doi.org/10.1016/j.precamres.2004.03.001.
- Barbosa, N.S., Teixeira, W., Bastos Leal, L.R., De Menezes Leal, A.B., 2013. Evolução crustal do setor ocidental do Bloco Arqueano Gavião, Cráton do São Francisco, com base em evidências U-Pb, Sm-Nd e Rb-Sr. Geol. USP Ser. Cient. 13, 63–88. https://doi.org/10.5327/Z1519-874X201300040004.
- Bauer, A.M., Fisher, C.M., Vervoort, J.D., Bowring, S.A., 2017. Coupled zircon Lu–Hf and U–Pb isotopic analyses of the oldest terrestrial crust, the >4.03 Ga Acasta Gneiss Complex. Earth Planet. Sci. Lett. 458, 37–48. https://doi.org/10.1016/j. epsl.2016.10.036.
- Bennett, V.C., Nutman, A.P., McCulloch, M.T., 1993. Nd isotopic evidence for transient, highly depleted mantle reservoirs in the early history of the Earth. Earth Planet. Sci. Lett. 119, 299–317. https://doi.org/10.1016/0012-821X(93)90140-5.
- Bleeker, W., 2003. The late Archean record: a puzzle in ca. 35 pieces. Lithos 71 (2–4), 99–134.

- Blichert-Toft, J., 2008. The Hf isotopic composition of zircon reference material 91500. Chem. Geol. 253, 252–257. https://doi.org/10.1016/j.chemgeo.2008.05.014.
- Bouvier, A., Vervoort, J.D., Patchett, P.J., 2008. The Lu–Hf and Sm–Nd isotopic composition of CHUR: constraints from unequilibrated chondrites and implications for the bulk composition of terrestrial planets. Earth and Planetary Science Letters 273 (1–2), 48–57.
- Bowring, S.A., Housh, T.B., 1995. The Earth's early Evolution. Am. Assoc. Adv. Sci. 269, 1535–1540.
- Cawood, P.A., Hawkesworth, C.J., Dhuime, B., 2013. The continental record and the generation of continental crust. Bull. Geol. Soc. Am. 125, 14–32. https://doi.org/ 10.1130/B30722.1
- Cawood, P.A., Chowdhury, P., Mulder, J.A., Hawkesworth, C.J., Capitanio, F.A., Gunawardana, P.M., Nebel, O., 2022. Secular Evolution of Continents and the Earth System. Rev. Geophys. 60. https://doi.org/10.1029/2022RG000789 e2022RG000789.
- Condie, K.C., 2000. Episodic continental growth models: Afterthoughts and extensions. Tectonophysics 322, 153–162. https://doi.org/10.1016/S0040-1951(00)00061-5.
- Condie, K.C., Aster, R.C., 2010. Episodic zircon age spectra of orogenic granitoids: the supercontinent connection and continental growth. Precambrian Res. 180, 227–236. https://doi.org/10.1016/J.PRECAMRES.2010.03.008.
- da Silva Filho, A.F., Guimarães, I.P., Van Schmus, W.R., 2002. Crustal evolution of the pernambuco-alagoas complex, Borborema Province, NE Brazil: Nd Isotopic Data from Neoproterozoic Granitoids. Gondwana Res. 5, 409–422. https://doi.org/ 10.1016/S1342-937X(05)70732-2.
- Dantas, E.L., Van Schmus, W.R., Hackspacher, P.C., Fetter, A.H., de Brito Neves, B.B., Cordani, U., Nutman, A.P., Williams, I.S., 2004. The 3.4–3.5 Ga São José do Campestre massif, NE Brazil: remnants of the oldest crust in South America. Precambrian Res. 130, 113–137. https://doi.org/10.1016/j.precamres.2003.11.002.
- Dantas, E.L., de Souza, Z.S., Wernick, E., Hackspacher, P.C., Martin, H., Xiaodong, D., Li, J.-W., 2013. Crustal growth in the 3.4–2.7 Ga São José de Campestre Massif, Borborema Province, NE Brazil. Precambrian Res Precambrian Accretionary Orogens 227, 120–156. https://doi.org/10.1016/j.precamres.2012.08.006.
- de Almeida, J., Dall'Agnol, R., de Oliveira, M.A., Macambira, M.J.B., Pimentel, M.M., Rämö, O.T., Guimaräes, F.V., Leite, A.A., 2011. Zircon geochronology, geochemistry and origin of the TTG suites of the Rio Maria granite-greenstone terrain: implications for the growth of the Archean crust of the Carajás province, Brazil. Precambrian Res. 187, 201–221. https://doi.org/10.1016/j.precamres.2011.03.004.
- Delgado, I., Fraga, L.M., Fuezi, V., Salvador, E.D., Fernandes, L.F.R., Santo, E.B.E., Cruz, R.D., Lopes, J.A., Moreira, A.P.C., 2021. Mapa integrado do Brasil ao Milionésimo. Brazilian Geological Survey - CPRM. https://rigeo.sgb.gov.br/handle/ doc/22527.
- dos Santos, C., Zincone, S.A., Queiroga, G.N., Bersan, S.M., Lana, C.C., Oliveira, E.P., 2022. Evidence for change in crust formation process during the Paleoarchean in the São Francisco Craton (Gavião Block): coupled zircon Lu-Hf and U-Pb isotopic analyses and tectonic implications. Precambrian Res. 368. https://doi.org/10.1016/ i.precamres.2021.106472.
- Fachetti, F.J.S., Fuck, R.A., Marimon, R.S., Ferreira, A., da Costa, A.C.D., Hawkesworth, C.J., 2024. Paleoarchean to Neoproterozoic crust formation and migmatization events in the Borborema Province, NE Brazil: Implications for the growth and reworking of the continental crust. Gondwana Res. 129, 75–90. https:// doi.org/10.1016/j.gr.2023.12.005.
- Ferreira, A., Dantas, E.L., Dos Santos, T.J.S., Fuck, R.A., Tedeschi, M., 2020. High-pressure metamorphic rocks in the Borborema Province, Northeast Brazil: reworking of Archean oceanic crust during proterozoic orogenies. Geosci. Front. 11, 2221–2242. https://doi.org/10.1016/j.gsf.2020.03.004.
- Fisher, C.M., Vervoort, J.D., 2018. Using the magmatic record to constrain the growth of continental crust—the Eoarchean zircon Hf record of Greenland. Earth Planet. Sci. Lett. 488, 79–91. https://doi.org/10.1016/j.epsl.2018.01.031.
- Fisher, C.M., Hanchar, J.M., Samson, S.D., Dhuime, B., Blichert-Toft, J., Vervoort, J.D., Lam, R., 2011. Synthetic zircon doped with hafnium and rare earth elements: A reference material for in situ hafnium isotope analysis. Chem. Geol. 286, 32–47. https://doi.org/10.1016/j.chemgeo.2011.04.013.
- Fisher, C.M., Vervoort, J.D., Hanchar, J.M., 2014. Guidelines for reporting zircon Hf isotopic data by LA-MC-ICPMS and potential pitfalls in the interpretation of these data. Chem. Geol. 363, 125–133. https://doi.org/10.1016/j.chemgeo.2013.10.019.
- Fisher, C.M., Bauer, A.M., Vervoort, J.D., 2020. Disturbances in the Sm-Nd isotope system of the Acasta Gneiss Complex—Implications for the Nd isotope record of the early Earth. Earth Planet. Sci. Lett. 530, 115900. https://doi.org/10.1016/j. epsl.2019.115900.
- Frost, C.D., McLaughlin, J.F., Frost, B.R., Fanning, C.M., Swapp, S.M., Kruckenberg, S.C., Gonzalez, J., 2017. Hadean origins of Paleoarchean continental crust in the Central Wyoming Province. Geol. Soc. Am. Bull. 129, 259–280. https://doi.org/10.1130/ B31555.1.
- Ganade de Araujo, C.E., Weinberg, R.F., Cordani, U.G., 2014. Extruding the Borborema Province (NE-Brazil): a two-stage Neoproterozoic collision process. Terra Nova 26, 157–168. https://doi.org/10.1111/ter.12084.
- Ganade, C.E., Weinberg, R.F., Caxito, F.A., Lopes, L.B.L., Tesser, L.R., Costa, I.S., 2021. Decratonization by rifting enables orogenic reworking and transcurrent dispersal of old terrains in NE Brazil. Sci. Rep. 11, 5719. https://doi.org/10.1038/s41598-021-84703-x.
- Gardiner, N.J., Johnson, T.E., Kirkland, C.L., Smithies, R.H., 2018. Melting controls on the lutetium–hafnium evolution of Archaean crust. Precambrian Res. 305, 479–488. https://doi.org/10.1016/j.precamres.2017.12.026.
- Groves, D.I., Santosh, M., 2021. Craton and thick lithosphere margins: the sites of giant mineral deposits and mineral provinces. Gondwana Res. 100, 195–222.

Guitreau, M., Blichert-Toft, J., Martin, H., Mojzsis, S.J., Albarède, F., 2012. Hafnium isotope evidence from Archean granitic rocks for deep-mantle origin of continental crust. Earth Planet. Sci. Lett. 337–338, 211–223. https://doi.org/10.1016/j.epsl.2012.05.029.

- Hammerli, J., Kemp, A.I.S., Whitehouse, M.J., 2019. In situ trace element and Sm-Nd isotope analysis of accessory minerals in an Eoarchean tonalitic gneiss from Greenland: Implications for Hf and Nd isotope decoupling in Earth's ancient rocks. Chem. Geol. 524, 394–405. https://doi.org/10.1016/j.chemgeo.2019.06.025.
- Hawkesworth, C., Cawood, P., Kemp, T., Storey, C., Dhuime, B., 2009. Geochemistry: A matter of preservation. Science 323, 49–50. https://doi.org/10.1126/ SCIENCE.1168549.
- Harrison, T.M., Blichert-Toft, J., Muller, W., Albarede, F., Holden, P., Mojzsis, S.J., 2005. Heterogeneous Hadean Hafnium: evidence of continental crust at 4.4 to 4.5 Ga. Science 310 (5756), 1947–1950.
- Hawkesworth, C., Cawood, P., Dhuime, B., 2013. Continental growth and the crustal record. Tectonophysics 609, 651–660. https://doi.org/10.1016/j.tecto.2013.08.013.
- Hawkesworth, C.J., Cawood, P.A., Dhuime, B., Kemp, T.I.S., 2017. Earth's continental lithosphere through time. Annu. Rev. Earth Planet. Sci. 45, 169–198. https://doi. org/10.1146/annurey-earth-063016-020525.
- Hoffmann, J.E., Münker, C., Polat, A., König, S., Mezger, K., Rosing, M.T., 2010. Highly depleted Hadean mantle reservoirs in the sources of early Archean arc-like rocks, Isua supracrustal belt, southern West Greenland. Geochim. Cosmochim. Acta 74, 7236–7260. https://doi.org/10.1016/j.gca.2010.09.027.
- Hoffmann, J.E., Kröner, A., Hegner, E., Viehmann, S., Xie, H., Iaccheri, L.M., Schneider, K.P., Hofmann, A., Wong, J., Geng, H., Yang, J., 2016. Source composition, fractional crystallization and magma mixing processes in the 3.48–3.43 Ga Tsawela tonalite suite (Ancient Gneiss Complex, Swaziland) – Implications for Palaeoarchaean geodynamics. Precambrian Res 276, 43–66.
- Hoffmann, J.E., Mu, C., Polat, A., Rosing, M.T., Schulz, T., 2011. The origin of decoupled Hf Nd isotope compositions in Eoarchean rocks from southern West Greenland, 75, pp. 6610–6628. https://doi.org/10.1016/j.gca.2011.08.018.
- Iizuka, T., Komiya, T., Johnson, S.P., Kon, Y., Maruyama, S., Hirata, T., 2009. Reworking of Hadean crust in the Acasta gneisses, northwestern Canada: evidence from in-situ Lu–Hf isotope analysis of zircon. Chem. Geol. 259, 230–239. https://doi.org/ 10.1016/j.chemgeo.2008.11.007.
- Jackson, S.E., Pearson, N.J., Griffin, W.L., Belousova, E.A., 2004. The application of laser ablation-inductively coupled plasma-mass spectrometry to in situ U – Pb zircon. geochronology 211, 47–69. https://doi.org/10.1016/j.chemgeo.2004.06.017.
- Kemp, A.I.S., Wilde, S.A., Hawkesworth, C.J., Coath, C.D., Nemchin, A., Pidgeon, R.T., Vervoort, J.D., DuFrane, S.A., 2010. Hadean crustal evolution revisited: New constraints from Pb-Hf isotope systematics of the Jack Hills zircons. Earth Planet. Sci. Lett. 296, 45–56. https://doi.org/10.1016/j.epsl.2010.04.043.
- Kemp, A.I.S., Vervoort, J.D., Bjorkman, K.E., Iaccheri, L.M., 2017. Hafnium Isotope Characteristics of Palaeoarchaean Zircon OG1/OGC from the Owens Gully Diorite, Pilbara Craton, Western Australia. Geostand. Geoanal. Res. 41, 659–673. https://doi.org/10.1111/ggr.12182.
- Kemp, A.I.S., Whitehouse, M.J., Vervoort, J.D., 2019. Deciphering the zircon Hf isotope systematics of Eoarchean gneisses from Greenland: Implications for ancient crustmantle differentiation and Pb isotope controversies. Geochim. Cosmochim. Acta 250, 76–97. https://doi.org/10.1016/j.gca.2019.01.041.
- Kemp, A.I.S., Vervoort, J.D., Petersson, A., Smithies, R.H., Lu, Y., 2023. A linked evolution for granite-greenstone terrains of the Pilbara Craton from Nd and Hf isotopes, with implications for Archean continental growth. Earth Planet. Sci. Lett. 601, 117895. https://doi.org/10.1016/j.epsl.2022.117895.
- Laurent, O., Martin, H., Moyen, J.F., Doucelance, R., 2014. The diversity and evolution of late-Archean granitoids: evidence for the onset of "modern-style" plate tectonics between 3.0 and 2.5 Ga. LITHOS 205, 208–235. https://doi.org/10.1016/j. lithos 2014 06 012
- Laurent, O., Guitreau, M., Bruand, E., Moyen, J.-F., 2024. At the Dawn of Continents: Archean Tonalite-Trondhjemite-Granodiorite Suites. Elements 20, 174–179. https://doi.org/10.2138/gselements.20.3.174.
- Laurent, O., Zeh, A., 2015. A linear Hf isotope-age array despite different granitoid sources and complex Archean geodynamics: Example from the Pietersburg block (South Africa). Earth Planet. Sci. Lett. 430, 326–338. https://doi.org/10.1016/j. epsl.2015.08.028.
- Lopes, L.B.L., Ganade, C.E., Duarte Campos, L., Brilhante Rodrigues, J., Takenaka, Bianca, de Oliveira, L., Larizzatti, J.H., Shen, M., Gao, T., Xu, M., Zhou, Y., Yao, Z., 2021. Crustal reworking and Archean TTG generation in the South Gavião Block, São Francisco Craton Brazil. Precambrian Res. 363. https://doi.org/ 10.1016/j.precamres.2021.106333.
- Martin, H., 1993. The mechanisms of petrogenesis of the Archaean continental crust—Comparison with modern processes. Lithos. The evolving earth 30, 373–388. https://doi.org/10.1016/0024-4937(93)90046-F.
- Martins de Sousa, D.F., Oliveira, E.P., Amaral, W.S., Baldim, M.R., 2020. The Itabuna-Salvador-Curaçá Orogen revisited, São Francisco Craton, Brazil: new zircon U-Pb ages and Hf data support evolution from archean continental arc to paleoproterozoic crustal reworking during block collision. J. S. Am. Earth Sci. 104, 102826. https://doi.org/10.1016/j.jsames.2020.102826.
- McLennan, S.M., Taylor, S.R., 1982. Geochemical Constraints on the growth of the Continental Crust. J. Geol. 90, 347–361. https://doi.org/10.1086/628690.
- Medeiros, E.L.M., Cruz, S.C.P., Barbosa, J.S.F., Paquette, J.L., Peucat, J.J., Jesus, S.S., Barbosa, R.G., Brito, R.S.C.B., Carneiro, M.A., 2017. The Santa Izabel complex, Gavião Block, Brazil: components, geocronology, regional correlations and tectonic implications. J. S. Am. Earth Sci. 80, 66–94. https://doi.org/10.1016/j.jsames.2017.09.008.

Moreira, I. De C., Oliveira, E.P., Martins De Sousa, D.F., 2022. Evolution of the 3.65–2.58 Ga Mairi Gneiss complex, Brazil: Implications for growth of the continental crust in the S\u00e3o Francisco Craton. Geosci. Front. 13. https://doi.org/10.1016/j. orf/2022.101366

- Moyen, J.-F., 2011. The composite Archaean grey gneisses: Petrological significance, and evidence for a non-unique tectonic setting for Archaean crustal growth. Lithos 123, 21–36. https://doi.org/10.1016/j.lithos.2010.09.015.
- Moyen, J.F., Martin, H., 2012. Forty years of TTG research. Lithos 148, 312–336. https://doi.org/10.1016/j.lithos.2012.06.010.
- Moyen, J.F., Zeh, A., Cuney, M., Dziggel, A., Carrouée, S., 2021. The multiple ways of recycling Archaean crust: A case study from the ca. 3.1 Ga granitoids from the Barberton Greenstone Belt, South Africa. Precambrian Res 353, 105998. https://doi. org/10.1016/j.precamres.2020.105998.
- Mulder, J.A., Nebel, O., Gardiner, N.J., Cawood, P.A., Wainwright, A.N., Ivanic, T.J., 2021. Crustal rejuvenation stabilised Earth's first cratons. Nat. Commun. 12, 3535. https://doi.org/10.1038/s41467-021-23805-6.
- Næraa, T., Scherstén, A., Rosing, M.T., Kemp, A.I.S., Hoffmann, J.E., Kokfelt, T.F., Whitehouse, M.J., 2012. afnium isotope evidence for a transition in the dynamics of continental growth 3.2 Gyr ago. Nat 485, 627–630. https://doi.org/10.1038/ nature11140.
- Neves, S.P., 2003. Proterozoic history of the Borborema province (NE Brazil): Correlations with neighboring cratons and Pan-African belts and implications for the evolution of western Gondwana. Tectonics 22. https://doi.org/10.1029/2001TC001352
- Neves, S.P., 2015. Constraints from zircon geochronology on the tectonic evolution of the Borborema Province (NE Brazil): Widespread intracontinental Neoproterozoic reworking of a Paleoproterozoic accretionary orogen. J. S. Am. Earth Sci. 58, 150–164. https://doi.org/10.1016/j.jsames.2014.08.004.
- Pacheco Neves, S.P., 2021. Comparative geological evolution of the Borborema Province and São Francisco Craton (eastern Brazil): Decratonization and crustal reworking during West Gondwana assembly and implications for paleogeographic reconstructions. Precambrian Res. 355, 106119. https://doi.org/10.1016/j. precamres.2021.106119.
- Neves, B.B.B., Santos, T.J.S., Dantas, E.L., 2022. O Terreno Tectonoestratigráfico São Pedro: Oeste da Zona Transversal – Província Borborema. Geol. USP Sér. Científica 22, 45–69. https://doi.org/10.11606/issn.2316-9095.v22-197489.
- Nutman, A.P., Cordani, U.G., 1993. SHRIMP U-Pb zircon geochronology of Archaean granitoids from the Contendas-Mirante area of the São Francisco Craton, Bahia, Brazil. Precambrian Res. 63, 179–188. https://doi.org/10.1016/0301-9268(93) 90032-W
- Oliveira, E.P., McNaughton, N.J., Zincone, S.A., Talavera, C., 2020. Birthplace of the São Francisco Craton, Brazil: evidence from 3.60 to 3.64 Ga Gneisses of the Mairi Gneiss complex. Terra Nova 32, 281–289. https://doi.org/10.1111/ter.12460.
- Paces, J.B., Miller, J.D., 1993. Precise U-Pb ages of Duluth complex and related mafic intrusions, northeastern Minnesota: geochronological insights to physical, petrogenetic, paleomagnetic, and tectonomagmatic processes associated with the 1.1 Ga Midcontinent Rift System. J. Geophys. Res. Solid Earth 98, 13997–14013. https://doi.org/10.1029/93.JB01159.
- Paquette, J.L., Barbosa, J.S.F., Rohais, S., Cruz, S.C.P., Goncalves, P., Peucat, J.J., Leal, A. B.M., Santos-Pinto, M., Martin, H., 2015. The geological roots of South America: 4.1Ga and 3.7Ga zircon crystals discovered in N.E. Brazil and N.W Argentina. Precambrian Res. 271, 49–55. https://doi.org/10.1016/j.precamres.2015.09.027.
- Patchett, P.J., Arndt, N.T., 1986. Nd isotopes and tectonics of 1.9-1.7 Ga crustal genesis. Earth Planet. Sci. 78 (4), 329–338.
- Paton, C., Woodhead, J.D., Hellstrom, J.C., Hergt, J.M., Greig, A., Maas, R., 2010. Improved laser ablation U-Pb zircon geochronology through robust downhole fractionation correction. Geochem. Geophys. Geosyst. 11. https://doi.org/10.1029/ 2009GC002618
- Paton, C., Hellstrom, J., Paul, B., Woodhead, J., Hergt, J., 2011. Iolite: Freeware for the visualisation and processing of mass spectrometric data. J. Anal. At. Spectrom. 26, 2508–2518. https://doi.org/10.1039/c1ja10172b.
- Petersson, A., Kemp, A.I.S., Gray, C.M., Whitehouse, M.J., 2020. Formation of early Archean Granite-Greenstone Terrains from a globally chondritic mantle: Insights from igneous rocks of the Pilbara Craton Western Australia. Chem. Geol. 551, 119757. https://doi.org/10.1016/j.chemgeo.2020.119757.
- Pitarello, M.Z., Santos, T.J.S., Ancelmi, M.F., 2019. Syn-to post-depositional processes related to high grade metamorphic BIFs: Geochemical and geochronological evidences from a Paleo to Neoarchean (3.5–2.6 Ga) terrain in NE Brazil. J. S. Am. Earth Sci. 96, 102312. https://doi.org/10.1016/j.jsames.2019.102312.
- Salerno, Ross, Vervoort, J.D., Fisher, C.M., Kemp, A.I.S., Roberts, N.M.W., 2021. The coupled Hf-Nd isotope record of the early Earth in the Pilbara Craton. Earth Planet. Sci. Lett. 572, 117139. https://doi.org/10.1016/j.epsl.2021.117139.
- Santos, F.G., Cavalcanti Neto, M.T.O., Ferreira, V.P., Bertotti, A.L., 2020. Eo to Paleoarchean metamafic-ultramafic rocks from the central portion of the Rio Grande do Norte Domain, Borborema Province, Northeast Brazil: the oldest south American platform rocks. J. S. Am. Earth Sci. 97, 102410. https://doi.org/10.1016/j. jsames.2019.102410.
- Santos-Pinto, M., Peucat, J.J., Martin, H., Barbosa, J.S.F., Fanning, C.M., Cocherie, A., Paquette, J.L., 2012. Crustal evolution between 2.0 and 3.5 Ga in the southern Gavião block (Umburanas-Brumado-Aracatu region), São Francisco Craton, Brazil: A 3.5-3.8 Ga proto-crust in the Gavião block? J. S. Am. Earth Sci. 40, 129–142. https://doi.org/10.1016/j.jsames.2012.09.004.
- Scherer, E., Munker, C., Mezger, K., 2001. Calibration of the lutetium-hafnium clock. Science 293 (5530), 683–687.
- Schmitt, R.S., Fragoso, R.A., Collins, A.S., 2018. Suturing Gondwana in the Cambrian: The orogenic events of the final amalgamation. In: Geology of Southwest Gondwana,

- 1° ed. Springer International Publishing, pp. 411–432. https://doi.org/10.1007/978.3.319.68920.3.15
- Sláma, J., Košler, J., Condon, D.J., Crowley, J.L., Gerdes, A., Hanchar, J.M., Horstwood, M.S.A., Morris, G.A., Nasdala, L., Norberg, N., Schaltegger, U., Schoene, B., Tubrett, M.N., Whitehouse, M.J., 2008. Plešovice zircon — A new natural reference material for U–Pb and Hf isotopic microanalysis. Chem. Geol. 249, 1–35. https://doi.org/10.1016/j.chemgeo.2007.11.005.
- Söderlund, U., Patchett, P.J., Vervoort, J.D., Isachsen, C.E., 2004. The 176Lu decay constant determined by Lu–Hf and U–Pb isotope systematics of Precambrian mafic intrusions. Earth and Planetary Science Letters 219 (3–4), 311–324.
- Steenberg, L., Boroughs, S., Knaack, C., 2017. Estimation of Accuracy And Precision For Trace Elements Analyzed By Inductively Coupled Plasma Mass Spectrometry (Icp-Ms) At The Peter Hooper Geoanalytical Laboratory. Washington State University. https://doi.org/10.1130/abs/2017AM-307211.
- Stern, R.A., Bodorkos, S., Kamo, S.L., Hickman, A.H., Corfu, F., 2009. Measurement of SIMS instrumental mass fractionation of Pb isotopes during zircon dating. Geostand. Geoanal. Res. 33, 145–168. https://doi.org/10.1111/j.1751-908X.2009.00023.x.
- Teixeira, W., Oliveira, E.P., Marques, L.S., 2017. Nature and Evolution of the Archean Crust of the São Francisco Craton, in: São Francisco Craton Eastern Brazil. Springer, Cham, pp. 29–56. https://doi.org/10.1007/978-3-319-01715-0_3.
- Vervoort, J.D., Kemp, A.I.S., 2016. Clarifying the zircon Hf isotope record of crust-mantle evolution. Chem. Geol. 425, 65–75. https://doi.org/10.1016/j. chemgeo.2016.01.023.

- Vervoort, J.D., Kemp, A.I., 2025. Isotope Evolution of the Depleted Mantle. Annu. Rev. Earth Planet. Sci. 53. https://doi.org/10.1146/annurev-earth-031621-112052.
- Vervoort, J.D., Kemp, T., Fisher, C.M., 2012. No significant production of continental crust prior to 3.8 Ga. AGU Fall Meet. Abstr. 2012, T11B–2570.
- Vervoort, J.D., Fisher, C.M., Kemp, A.I.S., 2013. The myth of a highly heterogeneous Hf-Nd eoarchean mantle and large early crustal volumes. Mineral. Mag. 77, 2409.
- Wang, D., Fisher, C.M., Vervoort, J.D., Cao, H., 2020. Nd isotope re-equilibration during high temperature metamorphism across an orogenic belt: evidence from monazite and garnet. Chem. Geol. 551, 119751. https://doi.org/10.1016/j. chemgeo.2020.119751.
- Wiedenbeck, M., Allé, P., Corfu, F., Griffin, W.L., Meier, M., Oberli, F., Quadt, A.V., Roddick, J.C., Spiegel, W., 1995. Three natural zircon standards for U-Th-Pb, Lu-Hf, trace element and REE analyses. Geostand. Geoanal. Res. 19, 1–23. https://doi.org/ 10.1111/j.1751-908X.1995.tb00147.x.
- Zeh, A., Gerdes, A., Barton, J.M., 2009. Archean Accretion and Crustal Evolution of the Kalahari Craton—the Zircon Age and Hf Isotope Record of Granitic Rocks from Barberton/Swaziland to the Francistown Arc. J. Petrol. 50, 933–966. https://doi. org/10.1093/petrology/egp027.
- Zincone, S.A., Oliveira, E.P., Laurent, O., Zhang, H., Zhai, M., 2016. 3.30 Ga high-silica intraplate volcanic-plutonic system of the Gavião Block, São Francisco Craton, Brazil: evidence of an intracontinental rift following the creation of insulating continental crust. Lithos 266–267, 414–434. https://doi.org/10.1016/j. lithos.2016.10.011.